Table 1. Inhibition of agonist-induced PAC1 binding by Sema3A

Agonist	Concentration (% inhibition)
ADP, μM	5 (90.4 ± 12.1)
PAR1-TRAP, μM	15 (115.2 ± 10.2)
Thrombin, U/mL	0.5 (97.4 ± 3.3)
U46619, μM	2 (112.5 ± 9.3)
Convulxin, ng/mL	5 (94.7 ± 6.0)
A23187, μM	2.5 (106 ± 5.5)
PMA, nM	200 (58.1 ± 14.3)

Platelets preincubated with 10 μg/mL Sema3A/Fc were activated with indicated agonists, and FITC-PAC1 binding was detected as demonstrated in Figure 2. Percent inhibition of mean fluorescent intensity against hIgG-treated platelets was calculated. Data represent mean ± SE of at least 3 independent experiments.

ADP and PAR1-TRAP stimulation, as well as PAC-1 binding (data not shown). PAC-1 binding with PT25-2, an anti-αIIbβ3 antibody that induces activated conformation of αIIbβ3 without intracellular signaling, was unaffected by preincubation with Sema3A (Figure 2C), indicating that Sema3A does not disturb PAC-1 binding competitively to its receptor. Since activation of αIIbβ3 leads to ligand binding and platelet aggregate formation, we studied the effects of Sema3A on platelet aggregation. Sema3A/AP impaired aggregate formation in low concentrations of collagen and thrombin (Figure 3), although it was hard to detect the inhibitory effects of Sema3A on platelet aggregation in high concentrations of the agonists.

Effects of Sema3A on granular secretion

We examined effects of Sema3A binding to platelets on granular secretion after ADP and thrombin stimulation. Surface expression of CD62P and CD63 was used for monitoring the secretion of alpha granule and dense or lysosome granule, respectively.[30] Sema3A/Fc dose-dependently inhibited surface expression of both CD62P and CD63 after ADP and thrombin stimulation without stirring, indicating that Sema3A inhibits aggregation-independent granule secretion induced by platelet agonists (Figure 4).

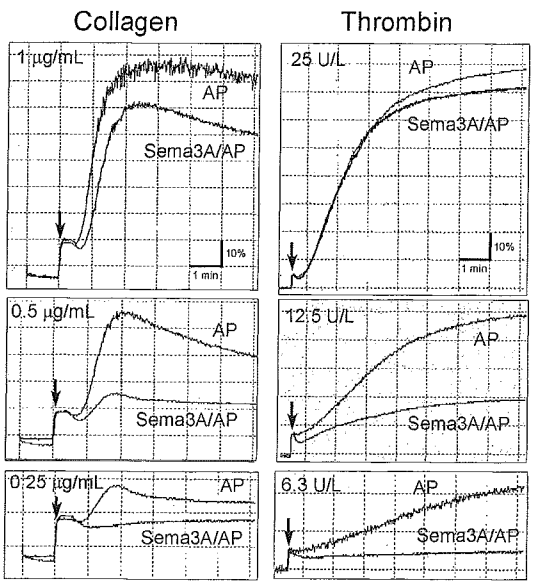

Figure 3. Inhibition of platelet aggregation by Sema3A. Washed platelets preincubated with 20 μg/mL Sema3A/AP or AP were activated with the indicated concentrations of collagen (left column) or thrombin (right column). Platelet aggregation was monitored using a platelet aggregometer. Arrow indicates the addition of agonists. Shown are representative results of 3 independent experiments.

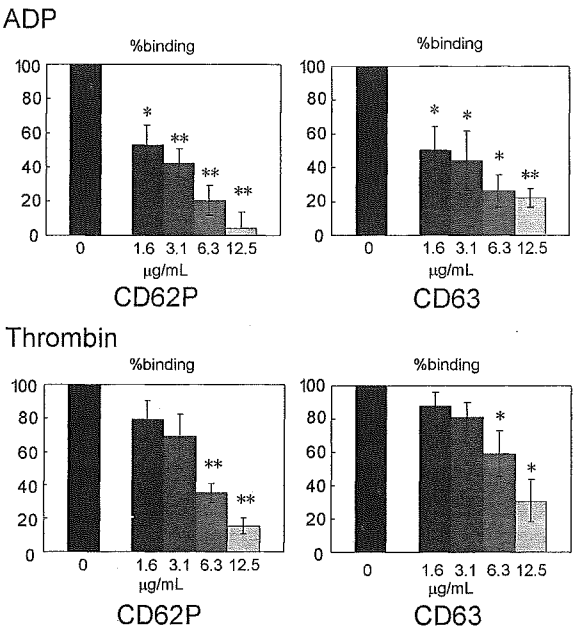

Figure 4. Inhibition of agonist-induced granular secretion by Sema3A. Washed platelets were preincubated with the indicated concentrations Sema3A/Fc, and then activated with ADP (5 μM) or thrombin (0.5 U/mL). Granular secretion was assessed by FITC-CD62P and PE-CD63 binding to platelets, and percent binding against hIgG-treated platelets was calculated. Shown are mean ± SE of percent binding of 3 independent experiments. $^*P < .05$; $^{**}P < .01$.

Effects of Sema3A on platelet adhesion and spreading

We next examined the effects of Sema3A on platelet adhesion to immobilized fibrinogen or nonspecific glass coverslips under static conditions. Quantification of adhered platelets by acid phosphatase method showed that preincubation with 20 μg/mL Sema3A/Fc led to about 20% reduction in platelet adhesion at every concentration of fibrinogen examined (Figure 5A). Microscopic examination demonstrated that after 45 minutes of incubation on 20 μg/mL fibrinogen, more than 80% of platelets showed full spreading (Figure 5Bi). In sharp contrast, spreading of Sema3A-treated platelets was markedly impaired (Figure 5Bii). The inhibition of platelet spreading by Sema3A was not αIIbβ3 specific, since Sema3A also inhibited platelet spreading on noncoated glass coverslips (Figure 5Biii-iv).

Effects of Sema3A on agonist-induced cytoskeleton rearrangement of platelets

The remarkable inhibition of platelet spreading by Sema3A suggests that Sema3A affects cytoskeletal rearrangement of platelets. To address the hypothesis, we quantified F-actin contents in platelets using bodipy-phallacidin and flow cytometry. Thrombin and PAR1-TRAP induced elevation of F-actin as demonstrated,[28] and Sema3A significantly impaired the elevation of agonist-induced F-actin elevation (Figure 6A). Cofilin is a protein that promotes severing and depolymerization of F-actin,[31,32] and involvement of cofilin in Sema3A signaling has been demonstrated.[31] Therefore, we next examined phosphorylation of cofilin after PAR1-TRAP stimulation. Sema3A decreased the level of phosphorylated cofilin in both resting and PAR1-TRAP–stimulated platelets, suggesting that Sema3A may keep cofilin in the dephosphorylated, activated state and increase severing of F-actin (Figure 6B). Since phosphorylation of cofilin is regulated by LIM kinase,[31,32] an effecter of Rac-PAK signaling pathway,[33] and the involvement of

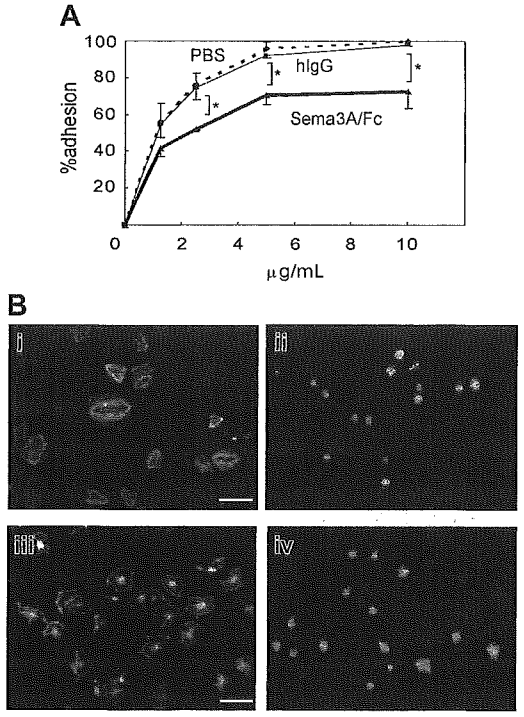

Figure 5. Effects of Sema3A on platelet adhesion and spreading. (A) Washed platelets were incubated with 20 μg/mL Sema3A/Fc (bold line) or hIgG (thin solid line), or PBS (dashed line), and then placed on the various concentrations of immobilized fibrinogen for one hour. After washing with PBS to remove nonadherent platelets, adhered platelets were quantified by acid phosphatase method. Mean and SE of percent adhesion of 3 independent experiments was plotted. $*P < .05$. (B) Sema3A-treated platelets (ii,iv) or hIgG-treated platelets (i,iii) were placed on fibrinogen-coated (i-ii) or nontreated (iii-iv) glass coverslips. Adhered platelets were stained with TRICT (tetramethylrhodamine-5(and 6)-isothiocyanate)–phalloidin. Images were captured with a CCD camera (DP-70; Olympus) mounted on an Olympus AX-80 fluorescence microscope equipped with a 100 ×/1.30 oil immersion objective lens. Images were acquired with Olympus DP Controller software and processed with Adobe Photoshop Elements 2.0 (Adobe Systems, San Jose, CA). Original magnification × 1000, and bar in panel Bi represents 10 μm.

Rac in semaphorin signaling is well demonstrated,[11,12] we examined the effects of Sema3A on Rac1 activation by PAR1-TRAP. Consistent with previous reports,[34,35] PAR1-TRAP induced rapid activation of Rac1 in platelets at the maximum in 30 seconds, and Sema3A almost completely inhibited the Rac1 activation induced by PAR1-TRAP (Figure 6C). These results suggest that Sema3A inhibits agonist-induced actin rearrangement via Rac1-dependent pathway including phosphorylation of cofilin.

Some reports demonstrated that Sema3A affects another cytoskeletal component, microtubule rearrangement.[36,37] However, we did not observe any apparent effects of Sema3A on tubulin staining in platelets (data not shown).

Effects of Sema3A on Ca^{2+} and cyclic nucleotide signaling in platelets

To examine whether Sema3A may affect Ca^{2+} signaling, fluo-3–loaded platelets were stimulated with thrombin and intracellular Ca^{2+} concentrations were monitored under flow cytometry. Thrombin induced rapid increase in intracellular Ca^{2+} concentrations in control platelets as described,[20] and Sema3A/Fc did not affect the thrombin-induced increase in intracellular Ca^{2+} concentrations (Figure 7).

Since the best characterized platelet inhibitory signaling pathways are cyclic nucleotide pathways,[38] we finally examined the effects of Sema3A on cyclic nucleotides in platelets. Sema3A did not increase the basal cAMP level in nonstimulated platelets per se (Table 2). Stable prostacyclin, iloprost, elevates intracellular cAMP, and addition of ADP impairs the iloprost-induced cAMP elevation by inhibiting adenylate cyclase.[39] Again, Sema3A treatment did not change cAMP contents in iloprost- and ADP-treated platelets (Table 2). Sema3A also had no effects on basal cGMP contents, whereas sodium nitroprusside, a stimulator of NO/protein kinase G pathway, induced elevation of cGMP contents (Table 3). Moreover, a nitric oxide synthase (NOS) inhibitor, L-nitroarginine methyl ester, or a NO-donor, L-arginine, had no effects on the inhibition of αIIbβ3 activation by Sema3A (data not shown).[40] These results suggest that neither cAMP nor cGMP is involved in inhibition of platelet function by Sema3A.

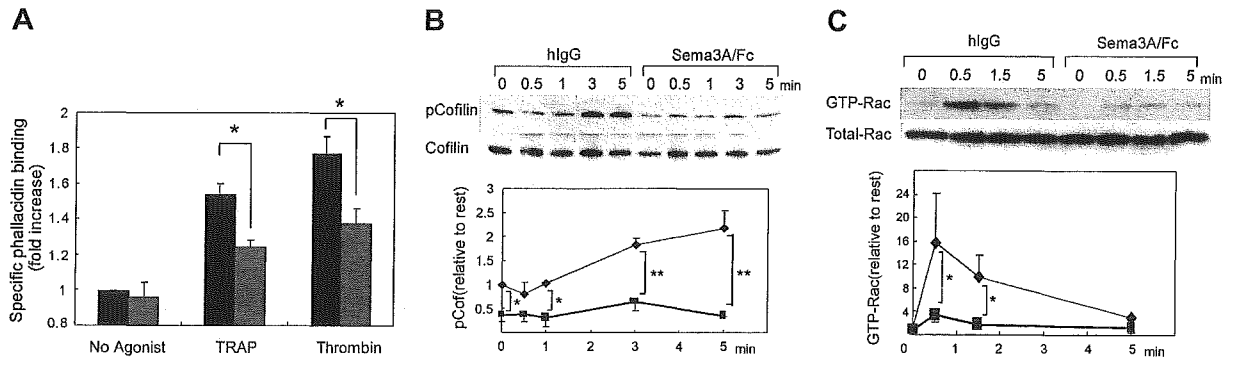

Figure 6. Effects of Sema3A on F-actin contents, cofilin phosphorylation, and Rac1 activation. (A) Sema3A/Fc- (gray bars) or hIgG-treated (black bars) platelets were activated by 30 μM PAR1-TRAP or 0.5 U/mL thrombin at 37°C for 30 seconds without stirring. After fixation, F-actin was stained with bodipy-phallacidin. Specific phallacidin binding was obtained by subtraction of FL1 fluorescence with a 300-fold more excess of unlabeled phallacidin from FL1 fluorescence without unlabeled phallacidin, and fold increase against fluorescence of no agonist sample was calculated. Data represent mean and SE of 3 independent experiments. $*P < .05$. (B) Sema3A/Fc- or hIgG-treated platelets were activated with 30 μM PAR1-TRAP for the indicated time at 37°C without stirring. Then, cells were lysed and SDS-PAGE was performed. Phospho-cofilin was detected by anti–phospho-cofilin–specific antibody. After stripping, total cofilin was detected by anticofilin antibody. Optical density of the bands was measured by NIH Image software, and relative increase against phospho-cofilin in IgG-treated platelets without thrombin was calculated. Mean and SE of 3 independent experiments was plotted in bottom panel. $*P < .05$; $**P < .01$. (C) Sema3A/Fc- or hIgG-treated platelets were activated with 30 μM PAR1-TRAP for the indicated time at 37°C without stirring. GTP-form of Rac1 was precipitated by incubation with GST-PAK1-PBD and glutathione beads. After SDS-PAGE electrophoresis, Rac1 was detected by a Rac1-specific antibody. Total Rac was detected by electrophoresis of total lysates on an SDS-PAGE gel followed by detection with the same antibody. Optical density of the bands was measured by NIH Image software, and relative increase against GTP-Rac in IgG-treated platelets without thrombin was calculated. Sema3A/Fc is indicated by ■ and bold lines; hIgG, by ◆ and thin lines. Mean and SE of 3 independent experiments was plotted in lower panel. $*P < .05$.

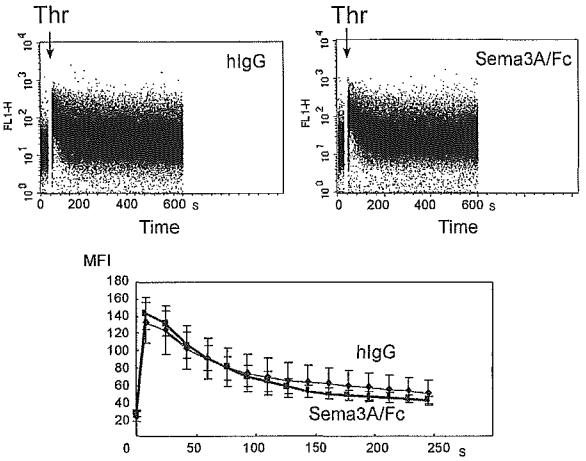

Figure 7. Effects of Sema3A on thrombin-induced increase of intracellular Ca^{2+} concentrations. Fluo-3–labeled platelets were incubated with 20 μg/mL Sema3A/Fc or hIgG. After the determination for about 10 seconds of baseline fluo-3 fluorescence from the platelet population, cell aspiration into the flow cytometry was briefly paused, and 1:10 volume of 5 U/mL thrombin (Thr) was added. The acquisition was then resumed, and changes in log fluorescence versus time were recorded (top panels). For each plot, rectangular analysis regions were defined over the time axis, and mean fluorescence intensity was calculated. Mean ± SE of 3 independent experiments was plotted in bottom panel. Bold and thin lines represent Sema3A/Fc and hIgG, respectively.

Discussion

In this report, we demonstrated for the first time the binding of Sema3A on platelets and extensive inhibitory effects of Sema3A on platelet function. As reported in endothelial cells,[16] Sema3A inhibited integrin-mediated function in platelets (ie, inhibition of αIIbβ3 activation and platelet aggregate formation, and adhesion and spreading on immobilized fibrinogen). However, Sema3A also inhibited αIIbβ3-independent adhesion and spreading on non-treated glass coverslips and aggregation-independent granular secretion. Although the most potent platelet inhibitory pathways are cyclic nucleotide pathways,[38] we did not detect any effect on cAMP and cGMP contents by Sema3A treatment. Thrombin-induced Ca^{2+} signaling was also unaffected by Sema3A treatment.

Sema3A markedly impaired αIIbβ3-independent as well as αIIbβ3-dependent platelet spreading. We demonstrated that Sema3A inhibited the increase of F-actin contents after thrombin or PAR1-TRAP stimulation. Thus, Sema3A inhibited adhesion-induced and agonist-induced actin rearrangement. Furthermore, Sema3A inhibited phosphorylation of cofilin and Rac1 activation after PAR1-TRAP stimulation. Several reports revealed that Rac1 activation is necessary for platelet actin assembly and lamellipodia formation after agonist stimulation.[34,35,41] Therefore, marked impairment of Rac1 activation is very likely to account for the Sema3A-induced impairment of actin rearrangement and spreading in platelets. There were 2 major downstream effectors of Rac1 identified, PAK and WAVEs ([Wiskott-Aldrich syndrome protein] WASP family Verprolin-homologous proteins).[42] Several PAK substrates or binding partners have been implicated in the effects of PAK, including filamin, LIM kinase, myosin, and paxillin.[43] Among them, LIM kinase phosphorylates and inactivates cofilin, a protein that promotes severing and depolymerization of F-actin.[31,32] Consistent with the inhibition of Rac1 activation, Sema3A inhibited phosphorylation of cofilin in both resting and activated platelets, suggesting that Sema3A increases severing and depolymerization of F-actin by keeping cofilin in the activated state. Rac1 inhibition by Sema3A might affect the activation of another major downstream effector of Rac1, WAVEs. WAVEs, also known as Scar, belong to the WASP family and activate actin-related protein 2 and 3 (Arp2/3) complex, resulting in nucleating actin polymerization.[43] Others and we have demonstrated that platelets contain WAVE isoforms and may regulate lamellipodia formation.[44,45] Therefore, it is also likely that Sema3A may inhibit actin rearrangement via inhibition of WAVE-dependent initiation of actin polymerization.

Table 2. Effects of Sema3A on cAMP

	cAMP, pmol/10^8 platelets
hIgG, 20 μg/mL	1.06 ± 0.19*
Sema3A/Fc, 20 μg/mL	1.00 ± 0.68*
Iloprost, 20 μg/L	45.94 ± 5.31
Iloprost, 20 μg/L + ADP, 5 μM + hIgG, 20 μg/mL	7.34 ± 0.47†
Iloprost, 20 μg/L + ADP, 5 μM + Sema3A/Fc, 20 μg/mL	5.66 ± 0.90†

Data represent the mean ± SE of 3 independent experiments.
*$P = .94$.
†$P = .24$.

Table 3. Effects of Sema3A on cGMP

	cGMP, pmol/10^8 platelets
hIgG, 20 μg/mL	0.83 ± 0.08*
Sema3A/Fc, 20 μg/mL	0.86 ± 0.04*
Sodium nitroprusside, 1 mM	5.56 ± 0.83

Data represent the mean ± SE of 3 independent experiments.
*$P = .70$.

In contrast to our results, it has been demonstrated that Rac1 activation is essential for Sema3A-induced growth cone collapse in neural cells,[46,47] and Sema3A-induced phosphorylation of cofilin is necessary for the process.[48] However, in these reports, the authors analyzed direct signaling induced by the binding of Sema3A. In this study, we analyzed the effects of Sema3A binding on agonist-induced signaling in platelets. Interestingly, Aizawa et al also found that phosphorylated cofilin was subsequently dephosphorylated within 5 minutes at the neural growth cone and the phosphorylated level of cofilin decreased to 0.16-fold of that of untreated growth cone,[48] which is consistent with our observation that cofilin is dephosphorylated in Sema3A-treated platelets. Signaling pathways from semaphorin receptors to Rac have not been fully understood even in neural cells.[11,12] Human plexin-B1, a receptor for Sema4D, and fly plexin B interact with activated Rac directly, and it has been suggested that these plexins sequester activated Rac and antagonize its signaling pathway.[49-51] Very recently Turner et al reported the association of activated Rac and the cytoplasmic tail of plexin-A1,[52] although others failed to detect the interaction.[50,53] Further studies are necessary to reveal the mechanism of regulation of Rac by Sema3A in platelets.

Is the impairment of actin rearrangement via inhibition of Rac1 responsible for Sema3A-induced extensive negative regulation of platelet function other than platelet spreading? To investigate the role of actin rearrangement on platelet function, effects of cytochalasins or latrunculin A, inhibitors of actin polymerization, have been studied.[54-58] There are some discrepancies in these reports, mainly because of the differences in experimental conditions; some reports demonstrated that high concentrations of cytochalasins inhibited agonist-induced αIIbβ3 activation and platelet aggregation, indicating that de novo actin polymerization affects activation of αIIbβ3,[54,55,58] whereas low concentrations of cytochalasin D and latrunculin A activated αIIbβ3.[57] Integrin activating inside-out

signaling consists of 2 aspects: conformational change that regulates integrin affinity and integrin clustering that regulates its avidity.[5,7] αIIbβ3 clustering may be promoted by actin cytoskeletal rearrangement, although conformational change seems to be the dominant way in αIIbβ3 activation.[59] Moreover, recent reports revealed that talin binding to integrin cytoplasmic tails is essential for integrin activation.[60,61] Since talin links integrin to actin filaments in clustering of integrins into adhesion complexes,[62,63] defects of actin polymerization may impair broad aspects of integrin signaling. However, impairment of actin rearrangement does not appear to be the sole mechanism of Sema3A inhibition of platelet function, since, in contrast to Sema3A, cytochalasins have no inhibitory effects on granular secretion.[55,58] Rac1 regulates many cellular activities besides cytoskeletal rearrangement, such as cell polarity and vesicle trafficking in other cells.[42] Moreover, Sema3A may act via Rac1-independent pathways (eg, the collapsin response mediator protein (CRMP)–mediated pathway).[12] These hypotheses remain to be determined.

It has been well documented that endothelial cells negatively regulate platelet function by secreted PGI_2, NO, and membrane-bound ecto-ADPase.[8] Since Sema3A is also produced in endothelial cells and inhibits platelet function extensively, Sema3A may contribute to maintain blood flow in normal, injured, or newly synthesized vessels by keeping platelets in the resting state. Moreover, since Sema3A appears to inhibit platelet function via unique Rac1-dependent pathway, modulation of Sema3A-inducing signaling pathway may be a new target of antiplatelet therapy.

In conclusion, we demonstrated that Sema3A binds to platelets and inhibits platelet function extensively. The inhibition of platelet function by Sema3A appeared to be mediated, at least in part, through impairment of agonist-induced Rac1-dependent actin rearrangement. We believe that these results reveal a new Sema3A function on thrombosis and hemostasis, and a unique inhibitory signaling pathway evoked by Sema3A binding to platelets.

Acknowledgment

We are grateful to Dr M. Moroi (Department of Protein Biochemistry, Institute of Life Science, Kurume University, Fukuoka, Japan) for providing us with convulxin.

References

1. Fuster V, Badimon L, Badimon JJ, Chesebro JH. The pathogenesis of coronary artery disease and the acute coronary syndromes. N Engl J Med. 1992;326:242-250.
2. Antithrombotic Trialists' Collaboration. Collaborative meta-analysis of randomised trials of antiplatelet therapy for prevention of death, myocardial infarction, and stroke in high risk patients. BMJ. 2002;324:71-86.
3. Savage B, Almus-Jacobs F, Ruggeri ZM. Specific synergy of multiple substrate-receptor interactions in platelet thrombus formation under flow. Cell. 1998;94:657-666.
4. Tomiyama Y, Shiraga M, Shattil SJ. Platelet membrane proteins as adhesion receptors. In: Gresele P, Page C, Fuster V, Vermylem J, eds. Platelets in Thrombotic and Non-Thrombotic Disorders. Cambridge, United Kingdom: Cambridge University Press; 2002:80-92.
5. Shattil SJ, Kashiwagi H, Pampori N. Integrin signaling: the platelet paradigm. Blood. 1998;91:2645-2657.
6. Tomiyama Y. Glanzmann thrombasthenia: integrin αIIbβ3 deficiency. Int J Hematol. 2000;72:448-454.
7. Shattil SJ, Newman PJ. Integrins: dynamic scaffolds for adhesion and signaling in platelets. Blood. 2004;104:1606-1615.
8. Pearson JD. Endothelial cell function and thrombosis. Baillieres Best Pract Res Clin Haematol. 1999;12:329-341.
9. Pasterkamp RJ, Kolodkin AL. Semaphorin junction: making tracks toward neural connectivity. Curr Opin Neurobiol. 2003;13:79-89.
10. Kolodkin AL, Levengood DV, Rowe EG, Tai YT, Giger RJ, Ginty DD. Neuropilin is a semaphorin III receptor. Cell. 1997;90:753-762.
11. Tamagnone L, Comoglio PM. Signalling by semaphorin receptors: cell guidance and beyond. Trends Cell Biol. 2000;10:377-383.
12. Goshima Y, Ito T, Sasaki Y, Nakamura F. Semaphorins as signals for cell repulsion and invasion. J Clin Invest. 2002;109:993-998.
13. Antipenko A, Himanen JP, van Leyen K, et al. Structure of the semaphorin-3A receptor binding module. Neuron. 2003;39:589-598.
14. Behar O, Golden JA, Mashimo H, Schoen FJ, Fishman MC. Semaphorin III is needed for normal patterning and growth of nerves, bones and heart. Nature. 1996;383:525-528.
15. Taniguchi M, Yuasa S, Fujisawa H, et al. Disruption of semaphorin III/D gene causes severe abnormality in peripheral nerve projection. Neuron. 1997;19:519-530.
16. Serini G, Valdembri D, Zanivan S, et al. Class 3 semaphorins control vascular morphogenesis by inhibiting integrin function. Nature. 2003;424:391-397.
17. Barberis D, Artigiani S, Casazza A, et al. Plexin signaling hampers integrin-based adhesion, leading to Rho-kinase independent cell rounding, and inhibiting lamellipodia extension and cell motility. FASEB J. 2004;18:592-594.
18. Honda S, Tomiyama Y, Aoki T, et al. Association between ligand-induced conformational changes of integrin $\alpha_{IIb}\beta_3$ and $\alpha_{IIb}\beta_3$-mediated intracellular Ca^{2+} signaling. Blood. 1998;92:3675-3683.
19. Tomiyama Y, Tsubakio T, Piotrowicz RS, Kurata Y, Loftus JC, Kunicki TJ. The Arg-Gly-Asp (RGD) recognition site of platelet glycoprotein IIb-IIIa on nonactivated platelets is accessible to high-affinity macromolecules. Blood. 1992;79:2303-2312.
20. Shiraga M, Tomiyama Y, Honda S, et al. Involvement of Na^+/Ca^{2+} exchanger in inside-out signaling through the platelet integrin $\alpha_{IIb}\beta_3$. Blood. 1998;92:3710-3720.
21. Kashiwagi H, Honda S, Tomiyama Y, et al. A novel polymorphism in glycoprotein IV (replacement of proline-90 by serine) predominates in subjects with platelet GPIV deficiency. Thromb Haemost. 1993;69:481-484.
22. Kashiwagi H, Tomiyama Y, Tadokoro S, et al. A mutation in the extracellular cysteine-rich repeat region of the β_3 subunit activates integrins $\alpha_{IIb}\beta_3$ and $\alpha_v\beta_3$. Blood. 1999;93:2559-2568.
23. Kashiwagi H, Shiraga M, Honda S, et al. Activation of integrin $\alpha_{IIb}\beta_3$ in the glycoprotein Ib-high population of a megakaryocytic cell line, CMK, by inside-out signaling. J Thromb Haemost. 2004;2:177-186.
24. Kashiwagi H, Schwartz MA, Eigenthaler M, Davis KA, Ginsberg MH, Shattil SJ. Affinity modulation of platelet integrin $\alpha_{IIb}\beta_3$ by β_3-endonexin, a selective binding partner of the β_3 integrin cytoplasmic tail. J Cell Biol. 1997;137:1433-1443.
25. Hayashi S, Oshida M, Kiyokawa T, et al. Determination of activated platelets: evaluation of methodology and application for patients with idiopathic thrombocytopenic purpura. Rinsho Byori. 2001;49:1287-1292.
26. Kiyoi T, Tomiyama Y, Honda S, et al. A naturally occurring Tyr143Hisα_{IIb} mutation abolishes $\alpha_{IIb}\beta_3$ function for soluble ligands but retains its ability for mediating cell adhesion and clot retraction: comparison with other mutations causing ligand-binding defects. Blood. 2003;101:3485-3491.
27. Bellavite P, Andrioli G, Guzzo P, et al. A colorimetric method for the measurement of platelet adhesion in microtiter plates. Anal Biochem. 1994;216:444-450.
28. Leng L, Kashiwagi H, Ren XD, Shattil SJ. RhoA and the function of platelet integrin $\alpha_{IIb}\beta_3$. Blood. 1998;91:4206-4215.
29. do Ceu Monteiro M, Sansonetty F, Goncalves MJ, O'Connor JE. Flow cytometric kinetic assay of calcium mobilization in whole blood platelets using Fluo-3 and CD41. Cytometry. 1999;35:302-310.
30. Rendu F, Brohard-Bohn B. Platelet organelles. In: Gresele P, Page C, Fuster V, Vermylem J, eds. Platelets in Thrombotic and Non-Thrombotic Disorders. Cambridge, United Kingdom: Cambridge University Press; 2002:104-112.
31. Arber S, Barbayannis FA, Hanser H, et al. Regulation of actin dynamics through phosphorylation of cofilin by LIM-kinase. Nature. 1998;393:805-809.
32. Yang N, Higuchi O, Ohashi K, et al. Cofilin phosphorylation by LIM-kinase 1 and its role in Rac-mediated actin reorganization. Nature. 1998;393:809-812.
33. Edwards DC, Sanders LC, Bokoch GM, Gill GN. Activation of LIM-kinase by Pak1 couples Rac/Cdc42 GTPase signalling to actin cytoskeletal dynamics. Nat Cell Biol. 1999;1:253-259.
34. Azim AC, Barkalow K, Chou J, Hartwig JH. Activation of the small GTPases, rac and cdc42, after ligation of the platelet PAR-1 receptor. Blood. 2000;95:959-964.
35. Vidal C, Geny B, Melle J, Jandrot-Perrus M, Fontenay-Roupie M. Cdc42/Rac1-dependent activation of the p21-activated kinase (PAK) regulates human platelet lamellipodia spreading: implication of the cortical-actin binding protein cortactin. Blood. 2002;100:4462-4469.
36. Fritsche J, Reber BF, Schindelholz B, Bandtlow CE. Differential cytoskeletal changes during growth cone collapse in response to hSema III and thrombin. Mol Cell Neurosci. 1999;14:398-418.
37. Gu Y, Ihara Y. Evidence that collapsin response mediator protein-2 is involved in the dynamics of

microtubules. J Biol Chem. 2000;275:17917-17920.

38. Schwarz UR, Walter U, Eigenthaler M. Taming platelets with cyclic nucleotides. Biochem Pharmacol. 2001;62:1153-1161.
39. Gabbeta J, Yang X, Kowalska MA, Sun L, Dhanasekaran N, Rao AK. Platelet signal transduction defect with Gα subunit dysfunction and diminished $G\alpha_q$ in a patient with abnormal platelet responses. Proc Natl Acad Sci U S A. 1997;94:8750-8755.
40. Freedman JE, Loscalzo J, Barnard MR, Alpert C, Keaney JF, Michelson AD. Nitric oxide released from activated platelets inhibits platelet recruitment. J Clin Invest. 1997;100:350-356.
41. Hartwig JH, Bokoch GM, Carpenter CL, et al. Thrombin receptor ligation and activated Rac uncap actin filament barbed ends through phosphoinositide synthesis in permeabilized human platelets. Cell. 1995;82:643-653.
42. Burridge K, Wennerberg K. Rho and Rac take center stage. Cell. 2004;116:167-179.
43. Takenawa T, Miki H. WASP and WAVE family proteins: key molecules for rapid rearrangement of cortical actin filaments and cell movement. J Cell Sci. 2001;114:1801-1809.
44. Oda A, Miki H, Wada I, et al. WAVE/Scars in platelets. Blood. Prepublished on August 3, 2004, as DOI 10.1182/blood-2003-04-1319. (Now available as Blood. 2005;105:3141-3148.
45. Kashiwagi H, Shiraga M, Kato H, et al. Expression and subcellular localization of WAVE isoforms in the megakaryocyte/platelet lineage. J Thromb Haemost.2005;3:361-368.
46. Jin Z, Strittmatter SM. Rac1 mediates collapsin-1-induced growth cone collapse. J Neurosci. 1997;17:6256-6263.
47. Kuhn TB, Brown MD, Wilcox CL, Raper JA, Bamburg JR. Myelin and collapsin-1 induce motor neuron growth cone collapse through different pathways: inhibition of collapse by opposing mutants of rac1. J Neurosci. 1999;19:1965-1975.
48. Aizawa H, Wakatsuki S, Ishii A, et al. Phosphorylation of cofilin by LIM-kinase is necessary for semaphorin 3A-induced growth cone collapse. Nat Neurosci. 2001;4:367-373.
49. Hu H, Marton TF, Goodman CS. Plexin B mediates axon guidance in Drosophila by simultaneously inhibiting active Rac and enhancing RhoA signaling. Neuron. 2001;32:39-51.
50. Vikis HG, Li W, He Z, Guan KL. The semaphorin receptor plexin-B1 specifically interacts with active Rac in a ligand-dependent manner. Proc Natl Acad Sci U S A. 2000;97:12457-12462.
51. Driessens MH, Hu H, Nobes CD, et al. Plexin-B semaphorin receptors interact directly with active Rac and regulate the actin cytoskeleton by activating Rho. Curr Biol. 2001;11:339-344.
52. Turner LJ, Nicholls S, Hall A. The activity of the plexin-A1 receptor is regulated by Rac. J Biol Chem. 2004;279:33199-33205.
53. Zanata SM, Hovatta I, Rohm B, Puschel AW. Antagonistic effects of Rnd1 and RhoD GTPases regulate receptor activity in semaphorin 3A-induced cytoskeletal collapse. J Neurosci. 2002;22:471-477.
54. Peerschke EI. Observations on the effects of cytochalasin B and cytochalasin D on ADP- and chymotrypsin-treated platelets. Proc Soc Exp Biol Med. 1984;175:109-115.
55. Lefebvre P, White JG, Krumwiede MD, Cohen I. Role of actin in platelet function. Eur J Cell Biol. 1993;62:194-204.
56. Torti M, Festetics ET, Bertoni A, Sinigaglia F, Balduini C. Agonist-induced actin polymerization is required for the irreversibility of platelet aggregation. Thromb Haemost. 1996;76:444-449.
57. Bennett JS, Zigmond S, Vilaire G, Cunningham ME, Bednar B. The platelet cytoskeleton regulates the affinity of the integrin $\alpha_{IIb}\beta_3$ for fibrinogen. J Biol Chem. 1999;274:25301-25307.
58. Natarajan P, May JA, Sanderson HM, Zabe M, Spangenberg P, Heptinstall S. Effects of cytochalasin H, a potent inhibitor of cytoskeletal reorganisation, on platelet function. Platelets. 2000;11:467-476.
59. Hato T, Pampori N, Shattil SJ. Complementary roles for receptor clustering and conformational change in the adhesive and signaling functions of integrin $\alpha_{IIb}\beta_3$. J Cell Biol. 1998;141:1685-1695.
60. Tadokoro S, Shattil SJ, Eto K, et al. Talin binding to integrin β tails: a final common step in integrin activation. Science. 2003;302:103-106.
61. Calderwood DA. Integrin activation. J Cell Sci. 2004;117:657-666.
62. Brown NH, Gregory SL, Rickoll WL, et al. Talin is essential for integrin function in Drosophila. Dev Cell. 2002;3:569-579.
63. Jiang G, Giannone G, Critchley DR, Fukumoto E, Sheetz MP. Two-piconewton slip bond between fibronectin and the cytoskeleton depends on talin. Nature. 2003;424:334-337.

Journal of Thrombosis and Haemostasis, 3: 2315–2323

ORIGINAL ARTICLE

Impaired platelet function in a patient with $P2Y_{12}$ deficiency caused by a mutation in the translation initiation codon

M. SHIRAGA,* S. MIYATA,† H. KATO,* H. KASHIWAGI,* S. HONDA,* Y. KURATA,‡ Y. TOMIYAMA* and Y. KANAKURA*

**Department of Hematology and Oncology, Graduate School of Medicine C9, Osaka University, Osaka, Japan; †Division of Blood Transfusion Medicine, National Cardiovascular Center, Osaka, Japan; and ‡Department of Blood Transfusion, Osaka University Hospital, Osaka, Japan*

To cite this article: Shiraga M, Miyata S, Kato H, Kashiwagi H, Honda S, Kurata Y, Tomiyama Y, Kanakura Y. Impaired platelet function in a patient with $P2Y_{12}$ deficiency caused by a mutation in the translation initiation codon. *J Thromb Haemost* 2005; **3**: 2315–23.

Summary. In this study, we have identified a patient (OSP-1) with a congenital $P2Y_{12}$ deficiency showing a mild bleeding tendency from her childhood and examined the role of $P2Y_{12}$ in platelet function. At low concentrations of agonists OSP-1 platelets showed an impaired aggregation to several kinds of stimuli, whereas at high concentrations they showed a specifically impaired platelet aggregation to adenosine diphosphate (ADP). ADP normally induced platelet shape change and failed to inhibit PGE_1-stimulated cAMP accumulation in OSP-1 platelets. Molecular genetic analysis revealed that OSP-1 was a homozygous for a mutation in the translation initiation codon (ATG to AGG) in the *P2Y*$_{12}$ gene. Heterologous cell expression of wild-type or mutant $P2Y_{12}$ confirmed that the mutation was responsible for the deficiency in $P2Y_{12}$. OSP-1 platelets showed a markedly impaired platelet spreading onto immobilized fibrinogen. Real-time observations of thrombogenesis under a high shear rate (2000 s^{-1}) revealed that thrombi over collagen were small and loosely packed and most of the aggregates were unable to resist against high shear stress in OSP-1. Our data suggest that secretion of endogenous ADP and subsequent $P2Y_{12}$-mediated signaling are critical for platelet aggregation, platelet spreading, and as a consequence, for stabilization of thrombus.

Keywords: $\alpha_{IIb}\beta_3$, initiation codon, mutation, $P2Y_{12}$ deficiency, platelets, thrombogenesis.

Introduction

Platelets play a crucial role not only in a hemostatic plug formation, but also in a pathologic thrombus formation, particularly within atherosclerotic arteries subjected to high shear stress [1,2]. As an initial step in thrombogenesis, platelets adhere to exposed subendothelial matrices such as von Willebrand factor (VWF) and collagen, then become activated and aggregate to each other. These processes are primarily mediated by platelet surface glycoproteins such as GPIb-IX-V, $\alpha_2\beta_1$, GPVI, and $\alpha_{IIb}\beta_3$ (GPIIb-IIIa) [3,4]. In addition, several mediators such as adenosine diphosphate (ADP), thromboxane A_2, and thrombin cause further platelet activation and recruitment of circulating platelets to the injury sites through activation of $\alpha_{IIb}\beta_3$ and subsequent binding of VWF and fibrinogen.

Recent studies have demonstrated a critical role for ADP in arterial thrombogenesis [5–7]. ADP is actively secreted from platelet dense granules on platelet activation and is passively released from damaged erythrocytes and endothelial cells. Platelets possess at least two major G protein-coupled ADP receptors that are largely responsible for platelet responses to ADP: $P2Y_1$ and $P2Y_{12}$ [6]. $P2Y_1$ is the G_q-coupled receptor responsible for mediating platelet shape change and reversible platelet aggregation through intracellular calcium mobilization [8,9], whereas $P2Y_{12}$ is the G_i-coupled receptor responsible for mediating inhibition of adenylyl cyclase and sustained platelet aggregation [10–12]. $P2Y_{12}$ is the therapeutic target of efficacious antithrombotic agents, such as ticlopidine, clopidogrel, and AR-C compounds [5,6], and its congenital deficiency results in a bleeding disorder [13,14]. The analyses of patients with $P2Y_{12}$ deficiency as well as $P2Y_{12}$-null mice would provide more precise information about the role of $P2Y_{12}$ in platelet function than those using $P2Y_{12}$ inhibitors. To date, four different families with a defect in the expression or the function of $P2Y_{12}$ have been characterized [10,13–16]. In this study, we have described a patient with the congenital $P2Y_{12}$ deficiency due to a homozygous mutation in the translation initiation codon and analyzed the role of $P2Y_{12}$ in platelet aggregation, platelet spreading onto immobilized fibrinogen, and thrombogenesis on a type I collagen-coated surface under a high shear rate. Our present data have demonstrated a crucial role of $P2Y_{12}$ in various platelet functions.

Correspondence: Yoshiaki Tomiyama, Department of Hematology and Oncology, Graduate School of Medicine C9, Osaka University, 2-2 Yamadaoka, Suita Osaka 565-0871, Japan.
Tel.: +81 6 6879 3821; fax: +81 6 6879 3879; e-mail: yoshi@hp-blood.med.osaka-u.ac.jp

Received 2 November 2004, accepted 7 June 2005

Materials and methods

Patient history

The proband (OSP-1) is a 67-year-old Japanese female with a lifelong history of easy bruising. She (OSP-1) was born from non-consanguineous parents who had no hemorrhagic diathesis. Although she showed massive bleeding during delivery of her son, she had no history of transfusions. Patient OSP-1 showed normal platelet count, normal coagulation tests (prothrombin time and activated partial thromboplastin time) and slightly elevated plasma fibrinogen (398 mg dL^{-1}). Ivy bleeding time of the patient was consistently prolonged (> 15 min). Clot retraction by MacFarlane's method was normal (50%; normal values 40%–70%). Her son never suffered from a bleeding tendency. Informed consent for analyzing their platelet function and molecular genetic abnormalities was obtained from OSP-1, her husband and their son.

Preparation of platelet-rich plasma and washed platelet suspension

Platelet-rich plasma (PRP) for aggregation studies was prepared by a centrifugation of whole blood anticoagulated with citrate at 250 *g* for 10 min and then the platelet count was adjusted at 300×10^6 mL^{-1} by platelet-poor plasma. Washed platelets were prepared as previously described [17]. In brief, 6 volumes of freshly drawn venous blood from the patient, her husband, son or healthy volunteers were mixed with 1 volume of acid–citrate–dextrose (ACD; National Institutes of Health Formula A, NIH, Bethesda, MD, USA) and centrifuged at 250 *g* for 10 min to obtain PRP. After incubation with 20 ng mL^{-1} prostaglandin E1 (PGE_1; Sigma-Aldrich, St Louis, MO, USA) for 15 min, the PRP was centrifuged at 750 *g* for 10 min, washed three times with 0.05 mol L^{-1} isotonic citrate buffer containing 20 ng mL^{-1} PGE_1 and resuspended in an appropriate buffer.

Platelet aggregometry

Platelet aggregation using PRP was monitored by a model PAM-6C platelet aggregometer (Mebanix, Tokyo, Japan) at 37 °C with a stirring rate of 1000 r.p.m. as previously described [18]. Protease-activated receptor 1-activating peptide (PAR1 TRAP, SFLLRNPNDKYEPF) and adenosine 3′,5′-diphosphate (A3P5P) were purchased from Sigma-Aldrich Corp. $P2Y_{12}$ antagonist, AR-C6993MX (2-propylthio-D-fluoromethylene adenosine 5-triphosphate) was a kind gift from AstraZeneca (Loughborough, UK).

Flow cytometry and measurement of intracellular cAMP

Flow cytometric analysis using various monoclonal antibodies (mAbs) specific for platelet membrane glycoproteins was performed as previously described [19].

For measuring intracellular cAMP levels, samples of 200 μL of washed platelets (60×10^6) in Walsh buffer (137 mM of NaCl, 2.7 mM of KCl, 1.0 mM of $MgCl_2$, 3.3 mM of NaH_2PO_4, 3.8 mM of HEPES, 0.1% of glucose, 0.1% of BSA, pH 7.4) were incubated with 1 μmol L^{-1} PGE_1 for 15 min, and then platelets were stimulated with ADP or epinephrine. After incubation for 15 min, total cellular cAMP levels were measured using the Biotrak cAMP enzyme immunoassay system from Amersham Pharmacia Biotech (Piscataway, NJ, USA).

Platelet adhesion assay

Adhesion study was performed as previously described [20]. In brief, non-treated polystyrene 10 cm dishes were coated with 100 μg mL^{-1} human fibrinogen in 5 mL of phosphate-buffered saline (PBS) at 4 °C overnight. After washing with PBS, dishes were blocked with PBS containing 1% of bovine serum albumin (BSA) for 90 min at 37 °C. Aliquots (1 mL) of washed platelets (25×10^6 mL^{-1}) were added to the fibrinogen-coated dishes and incubated at 37 °C. After incubation for 40 min, adherent platelets were fixed with 3.7% formaldehyde, permeabilized with 0.1% Triton X-100 and stained with TRITC-conjugated phalloidin. Platelet morphology and degrees of spreading were determined by fluorescence microscopy (Olympus, Tokyo, Japan).

Platelet thrombus formation under flow conditions

The real-time observation of mural thrombogenesis on a type I collagen-coated surface under a high shear rate (2000 s^{-1}) was performed as previously described [21]. In brief, type I collagen-coated glass coverslips were placed in a parallel plate flow chamber (rectangular type; flow path of 1.9-mm width, 31-mm length, and 0.1-mm height). The chamber was assembled and mounted on a microscope (BX60; Olympus, Tokyo, Japan) equipped with epifluorescent illumination (BX-FLA; Olympus) and a charge-coupled device (CCD) camera system (U-VPT-N; Olympus). Whole blood containing mepacrine-labeled platelets obtained from OSP-1 or control subjects was aspirated through the chamber by a syringe pump (Model CFV-3200, Nihon Kohden, Tokyo, Japan) at a constant flow rate of 0.285 mL min^{-1}, producing a wall shear rate of 2000 s^{-1} at 37 °C.

Amplification and analysis of platelet RNA

Total cellular RNA of platelets was isolated from 20 mL of whole blood, and $P2Y_1$ or $P2Y_{12}$ mRNA was specifically amplified by reverse transcription-polymerase chain reaction (RT-PCR), as previously described [22]. The following primers were constructed based on the published sequence of $P2Y_{12}$ cDNA and used for the first round PCR for $P2Y_{12}$ cDNA: Y12F1, 5′-GGCTGCAATAACTACTACTTACTGG-3′ [sense, nucleotide(nt) −74 to −50]; Y12R4, 5′-CAGGACAGTGTAGAGCAGTGG-3′ (antisense, nt 85 to 105) [10].

Allele-specific restriction enzyme analysis (ASRA)

Genomic DNA was isolated from mononuclear cells using SepaGene kit (Sanko Junyaku Co Ltd, Tokyo, Japan). Amplification of the region around the initiation codon of the $P2Y_{12}$ gene was performed by using primers *Bsr*DI-GF, 5′-CTTTTGTTCTCTAGGTAACCAACAAGCAA-3′ (sense, the mismatched base is underlined), and Y12R4 (antisense described above) using 250 ng of DNA as a template. These primers can be found in GenBank accession no. AC024886.20 and the sense primer corresponds to 127558–127585. PCR products were then digested with restriction enzyme *Bsr*DI. The resulting fragments were electrophoresed in a 6% polyacrylamide gel.

Construction of $P2Y_{12}$ expression vectors and cell transfection

The full-length cDNA of wild-type (WT) and mutant $P2Y_{12}$ was amplified by RT-PCR using primers Y12-*Hin*dIII-F, 5′-GAATTCAAGCTTCAAGAAATGCAAGCCGTCGACA-ACCTC-3′ (sense, nt −6 -21 for WT, *Eco*RI and *Hin*dIII sites introduced at the 5′ end were underlined) or Y12-*Hin*dIII-F2, 5′-GAATTCAAGCTTCAAGAAAGGCAAGCCGTCGAC-AACCTC-3′ (sense, nt −6 −21 for mutant), and Y12H-Not-R, 5′-TCTAGAGCGGCCGCTCAATGGTGATGGTGATGA-TGCATTGGAGTCTCTTCATT-3′ (antisense, nt 1012–1029, His × 6 were introduced before stop codon, *Not*I and *Xba*I sites introduced at the 5′ end were underlined). The amplified fragments were digested with *Hin*dIII and *Not*I, and the resulting 1059-bp fragments (nt −9 −1050) were extracted using QIAquick gel extraction kit (Qiagen, GmbH, Germany). These fragments were inserted into the pcDNA3 (Invitrogen, San Diego, CA, USA) digested with *Hin*dIII and *Not*I. The fragments inserted were characterized by sequence analysis to verify the absence of any other substitutions and the proper insertion of the PCR cartridge into the vector.

A total of 10 μg of WT or mutant $P2Y_{12}$ construct was transfected into human embryonic kidney 293 cells (HEK293 cells, 10^6 cells) using the calcium phosphate method as previously described [22]. Transfectants were lyzed by 1% Triton X-100 PBS containing protease inhibitors 2 days after transfection, and proteins were separated by 7.5% SDS-PAGE. After transferred onto a PVDF membrane, expressed proteins were detected by rabbit anti-His tag antibody.

Results

Platelet aggregation studies

We first examined the expression of platelet membrane glycoproteins in OSP-1 by flow cytometry. The patient's platelets (OSP-1 platelets) normally express GPIb-IX, $\alpha_{IIb}\beta_3$ (GPIIb-IIIa), $\alpha_2\beta_1$, and CD36 (data not shown). Fig. 1 shows platelet aggregation of PRP in response to various agonists. The aggregation of OSP-1 platelets induced by 20 μM of ADP was markedly impaired with only a small and transient

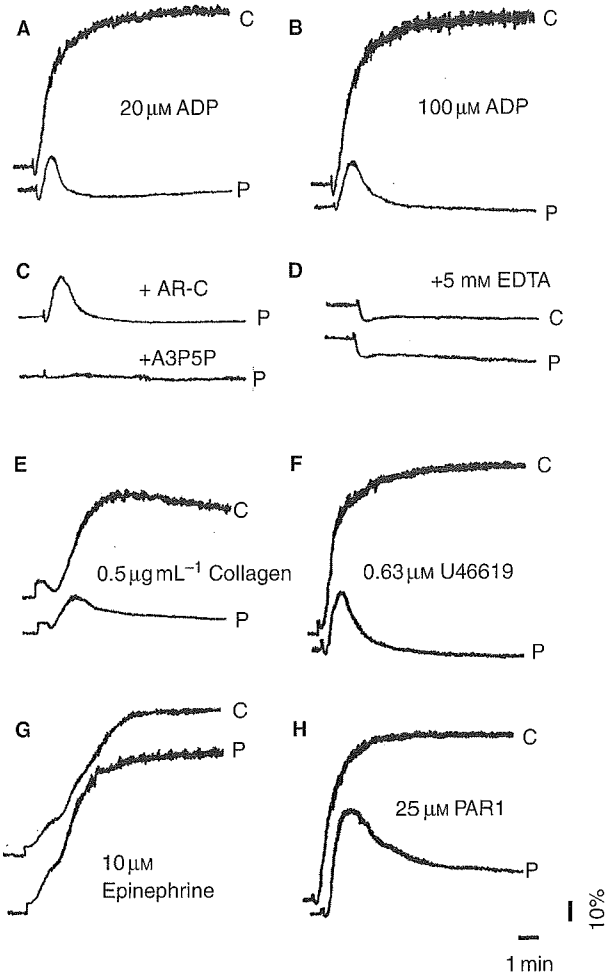

Fig. 1. Platelet aggregation induced by various agonists. Platelet aggregation was induced by various agonists in citrated PRP from patient OSP-1 (labeled 'P') or a control subject (labeled 'C'). Agonists used are (A) 20 μM of ADP, (B) 100 μM of ADP, (C) 20 μM of ADP in the presence of 1 μM of AR-C69931MX ('AR-C'), a specific $P2Y_{12}$-antagonist, or 1 mM of A3P5P ('A3P5P'), a specific $P2Y_1$-antagonist, (D) 20 μM of ADP in the presence of 5 mM of EDTA, (E) 0.5 μg mL^{-1} of collagen, (F) 0.63 μM of U46619, (G) 10 μM of epinephrine, and (H) 25 μM of PAR1-TRAP.

aggregation (Fig. 1A), and the aggregation was still impaired even at 100 μM of ADP (Fig. 1B). As compared with control platelets, the aggregation of OSP-1 platelets was also impaired with a transient aggregation in response to low concentrations of collagen (0.5 μg mL^{-1}, Fig. 1E), U46619 (0.63 μM, Fig. 1F), or PAR1 TRAP (25 μM, Fig. 1H). In response to 1.3 mg mL^{-1} ristocetin (not shown) or 10 μM of epinephrine (Fig. 1G), OSP-1 platelets aggregated normally. When OSP-1 platelets were stimulated with 20 μM of ADP in the presence of 5 mM of EDTA, the light transmission decreased equivalent to control platelets suggesting that OSP-1 platelets changed shape normally (Fig. 1D). We then examined effects of ADP receptor antagonists on the aggregation of OSP-1 platelets induced by 20 μM of ADP. A total of 1 mM of A3P5P, a specific $P2Y_1$ antagonist, abolished the residual response of OSP-1 platelets to ADP, whereas 1 μM of AR-C69931MX, a specific $P2Y_{12}$

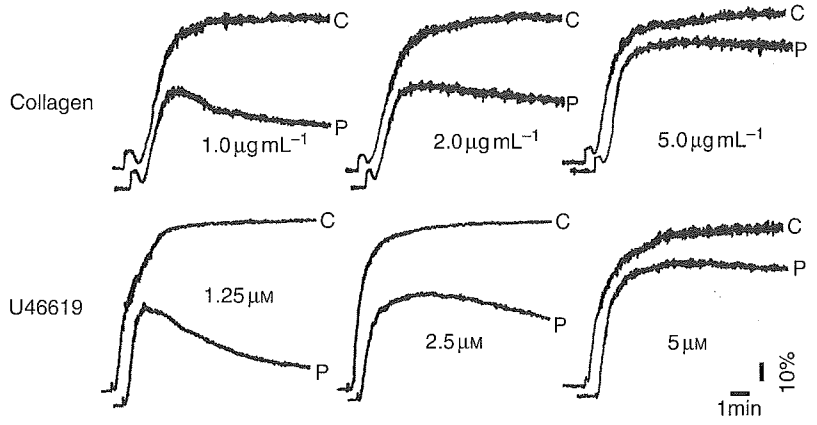

Fig. 2. Platelet aggragation induced by collagen or U46619 at various concentrations. Platelet aggregation in citrated PRP from patient OSP-1 (labeled 'P') or a control subject (labeled 'C') was induced by various concentrations of collagen or U46619. At high concentrations of collagen or U46619, OSP-1 platelets aggregate almost normally.

antagonist, did not induce an additional inhibition on the platelet aggregation (Fig. 1C). These data suggest that the impaired response of the patient's platelets may be due to an abnormality in signaling evoked by ADP and that $P2Y_{12}$-mediated signaling rather than $P2Y_1$-mediated signaling may be completely defective in patient OSP-1.

We also examined the aggregation of OSP-1 platelets induced by higher concentrations of agonists. As shown in Fig. 2, the aggregation response of OSP-1 platelets improved as the concentrations of agonists increased, and they aggregated almost normally in response to high concentrations of collagen (5 μg mL^{-1}), U46619 (5 μM), or PAR1 TRAP (100 μM) (not shown). In addition, we confirmed that 1 μM of AR-C69931MX conferred essentially the same defect on the aggregation of control platelets in response to U46619 as that of OSP-1 platelets and did not further inhibit OSP-1 platelet aggregation induced by 5 μg mL^{-1} of collagen, 5 μM of U46619, or 100 μM of PAR1 TRAP (data not shown). These data indicated that at high concentrations of agonists OSP-1 platelets showed the specifically impaired aggregation to ADP.

Effect of ADP on PGE_1-stimulated cAMP accumulation in platelets

To determine whether $P2Y_{12}$-mediated signaling is specifically impaired, we examined an inhibitory effect of ADP on 1 μM of PGE_1-stimulated cAMP accumulation in platelets from the patient, her husband, their son, and healthy unrelated controls. ADP inhibited intracellular cAMP levels in platelets from the patient's husband, son and healthy unrelated controls (not shown) by approximately 80%, whereas the inhibition was only 15% in the patient's platelets (Fig. 3). In contrast to ADP, epinephrine normally inhibited cAMP accumulation in platelets from the patient as well as her husband and son. These results strongly suggest that the defect could be due to an abnormality in G_i coupling ADP receptor, $P2Y_{12}$.

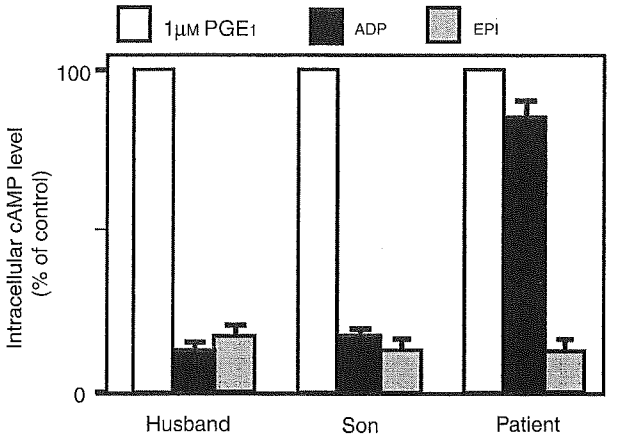

Fig. 3. Effect of ADP or epinephrine on the inhibition of PGE_1-induced cAMP accumulation in platelets. Washed platelets from patient OSP-1, husband or son were incubated with 1 μM of PGE_1 for 15 min and stimulated with 20 μM of ADP or 10 μM of epinephrine. Intracellular cAMP levels were expressed as a percent of cAMP levels in the absence of agonists. Results in OSP-1 are the mean of two experiments.

Nucleotide sequence analysis of cDNA and genomic DNA of $P2Y_{12}$

To reveal a molecular genetic defect in OSP-1, we analyzed the entire coding regions of both $P2Y_1$ and $P2Y_{12}$ cDNAs amplified from platelet mRNA by RT-PCR. A single nucleotide substitution (T → G) was identified within the translation initiation codon (ATG → AGG) in the patient's $P2Y_{12}$ cDNA (Fig. 4A). This substitution was also confirmed by reverse sequencing. No other nucleotide substitutions were detected within the coding region of either $P2Y_{12}$ or $P2Y_1$ cDNA from the patient. OSP-1 appeared homozygous for the substitution, and the substitution was not detected in 20 control subjects.

Nucleotide sequence analysis of PCR fragments from the patient's genomic DNA also suggested the homozygosity of the substitution (data not shown). To further confirm the homo-

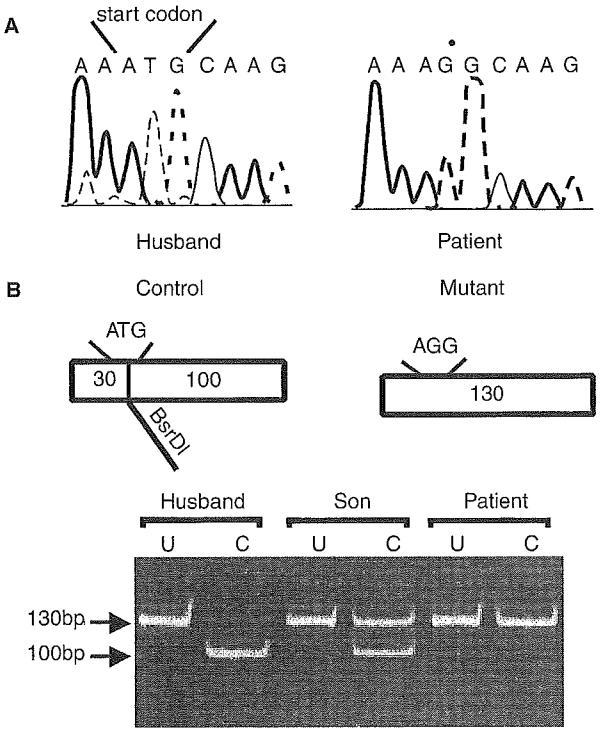

Fig. 4. Sequence analysis of $P2Y_{12}$ cDNA and restriction enzyme analysis of the $P2Y_{12}$ gene. (A) cDNA obtained by RT-PCR from platelet mRNA was analyzed by sequencing using a sense primer Y12F1. (B) PCR was performed to generate 130-bp fragments including initiation codon of $P2Y_{12}$ as described in Materials and methods. Undigested (U) or digested (C) PCR products with *Bsr*DI were analyzed on a 6% polyacrylamide gel. In patient OSP-1, the T → G mutation at position 2 abolishes a *Bsr*DI restriction site.

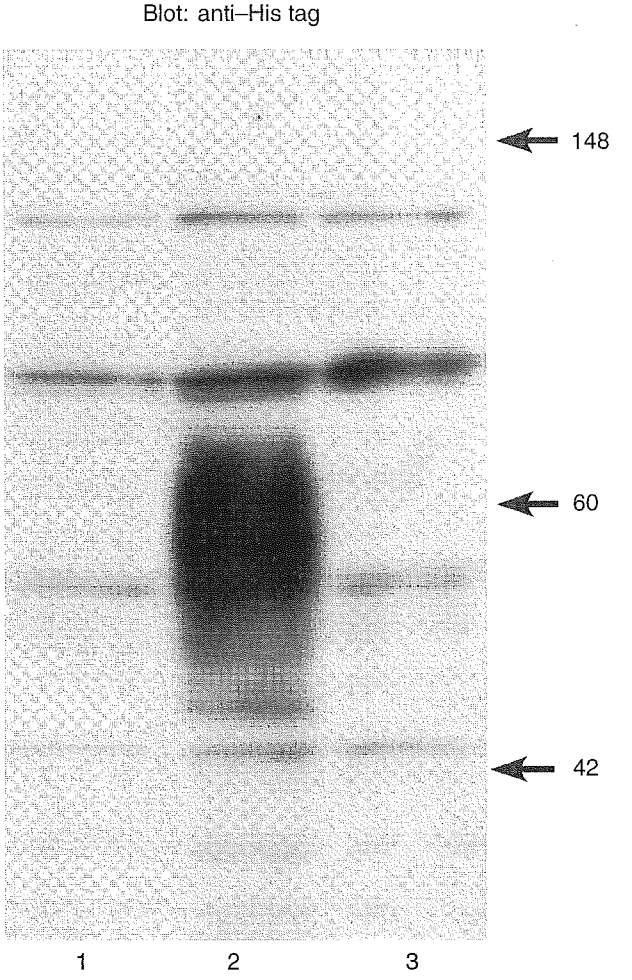

Fig. 5. Expression of $P2Y_{12}$ in HEK293 cells transfected with WT or mutant His-tag attached $P2Y_{12}$. Wild-type or mutant $P2Y_{12}$ construct was transfected into HEK293 cells using the calcium phosphate method. Transfectants were lyzed by 1% Triton X-100 PBS containing protease inhibitors 2 days after transfection. Cell lysates from mock transfectant (lane 1), cells transfected with WT $P2Y_{12}$ (lane 2) or mutant $P2Y_{12}$ (lane 3) were separated by 7.5% SDS-PAGE, and immunoblot was performed by anti-His-tag antibodies.

zygosity, allele-specific restriction enzyme analysis (ASRA) was performed. The region around the initiation codon of the $P2Y_{12}$ gene was amplified by PCR using primers *Bsr*DI-GF and Y12R4. A restriction site for *Bsr*DI would be abolished by the T → G substitution. As shown in Fig. 4B, ASRA clearly indicated that the patient and her son were homozygous and heterozygous for the substitution, respectively. These results also confirm that the substitution is inheritable.

Heterologous cell expression of WT and mutant $P2Y_{12}$

As the substitution at the translation initiation codon might induce an alternative translation starting at downstream ATGs leading to an expression of shorter form of $P2Y_{12}$, we decided to investigate effects of the substitution found in the patient on the expression of $P2Y_{12}$. Expression vectors encoding WT and mutant $P2Y_{12}$ in which His-tag was attached at the C-terminal portion of $P2Y_{12}$ were constructed as described in the Materials and methods. Wild-type or mutant $P2Y_{12}$ construct was transfected into HEK 293 cells, and then expressed proteins were analyzed 48 h after transfection in an immunoblot assay employing anti-His antibodies. As shown in Fig. 5, WT $P2Y_{12}$ protein with an apparent molecular weight of ~60 KDa was expressed in 293 cells as a His-tag-positive protein. In sharp contrast, the mutant $P2Y_{12}$-expression vector failed to express any His-tag-positive protein. These results provide strong evidence that the T → G substitution at the translation initiation codon of $P2Y_{12}$ cDNA is responsible for the $P2Y_{12}$ deficiency.

Platelet spreading on immobilized fibrinogen

As it has been well documented that release of endogenous ADP is required for full platelet spreading onto immobilized fibrinogen [23], we next analyzed the patient's platelet spreading in order to evaluate the role of $P2Y_{12}$. Control platelets adhered to fibrinogen underwent morphological changes ranging from filopodia protrusion to complete spreading, and 50.5% ± 21.3% of the adherent platelets spread ($n = 3$) (Fig. 6A). In sharp contrast, the patient's platelets showed an

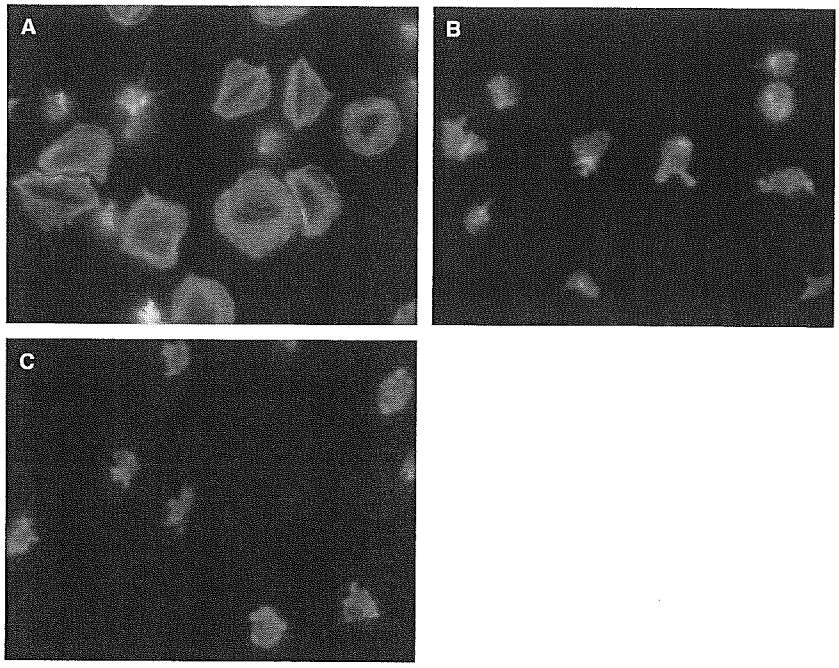

Fig. 6. Platelet spreading on immobilized fibrinogen. (A,B) Washed platelets from a control subject were applied onto fibrinogen-coated polystyrene dishes and incubated at 37 °C for 40 min without any inhibitor (A) or with 1 μM of AR-C69931MX (B). (C) Washed platelets from the patient were applied onto fibrinogen-coated polystyrene dishes and incubated at 37 °C for 40 min without any inhibitor. Adherent platelets were then fixed, permeabilized and stained with TRITC-conjugated phalloidin. Platelet morphology was analyzed by fluorescence microscopy.

impaired spreading and only 2.3% ± 1.4% of the adherent platelets spread ($n = 3$, $P < 0.001$, Fig. 6C). Similar results were obtained with control platelets in the presence of 1 μM of AR-C69931MX (6.2% ± 2.2%, $n = 3$, $P < 0.001$, Fig. 6B). In addition, 1 mM of A3P5P also markedly inhibited platelet spreading ($n = 3$, 10.1% ± 2.2%, $P < 0.001$, not shown). These results suggest that both $P2Y_{12}$ and $P2Y_1$ are necessary for platelet spreading.

Platelet-thrombus formation on immobilized collagen under flow conditions

To investigate the role of $P2Y_{12}$ in thrombus formation, we observed the real-time process of mural thrombogenesis on a type I collagen-coated surface under flow conditions with high shear rate (2000 s^{-1}) using the whole blood from OSP-1. Real-time observation revealed that thrombi formed on type I collagen were unstable. As platelet aggregates of the patient were loosely packed each other and unable to resist against high shear stress, most of the aggregates at the apex of the thrombi came off the thrombi constantly. On the other hand, most of thrombi formed by control platelets were densely packed with higher fluorescent intensity and were stable with constant growth during observation (Video 1 and 2).

As shown in Fig. 7A, the area covered with patient platelets after 7 min of flow was greater than that of control platelets (91.8% ± 0.3% vs. 82.2% ± 1.4%, $n = 3$, $P < 0.01$). However, thrombi formed by OSP-1 platelets were loosely packed, whereas thrombi were large and densely packed in controls. The overall fluorescent intensity of thrombi of OSP-1 platelets was lower than that of control platelets. Three-dimensional analysis revealed the striking difference in size and shape of individual thrombus formed after 10 min between the patient and control platelets (Fig. 7B). Thrombi formed by control platelets were large in size, clearly edged and surrounded by thrombus-free areas. On the other hand, individual thrombus formed by patient platelets was mostly small and appeared to be a thin layer of platelet aggregates. Thrombus height at the plateau phase was 10.2 ± 0.4 μm, which was less than half of controls (21.2 ± 0.4 μm).

Discussion

$P2Y_{12}$ coupled with $G\alpha_i$, primarily with $G\alpha_{i2}$, consists of 342 amino acid residues with seven transmembrane domains (TM), and its deficiency is responsible for congenital bleeding diathesis [10–16]. To date, five mutations responsible for a defect in the expression or the function of $P2Y_{12}$ in four different families have been demonstrated [10,15,16]. Patient ML possessed a mutation consisting of a two nucleotide deletion at amino acid 240 (near the N-terminal end of TM6), which would lead to a premature termination of $P2Y_{12}$ [10,14]. A two nucleotide deletions at amino acid 98 (next to the N-terminal end of TM3) and a single nucleotide deletion occurring just beyond TM3 were identified in other two families, both of which would lead to a premature termination of $P2Y_{12}$ [13,15]. However, in these reports expression studies had not been performed to show the direct association between these mutations and the $P2Y_{12}$ deficiency [10,15]. Patient AC, whose platelets expressed dysfunctional $P2Y_{12}$ with normal

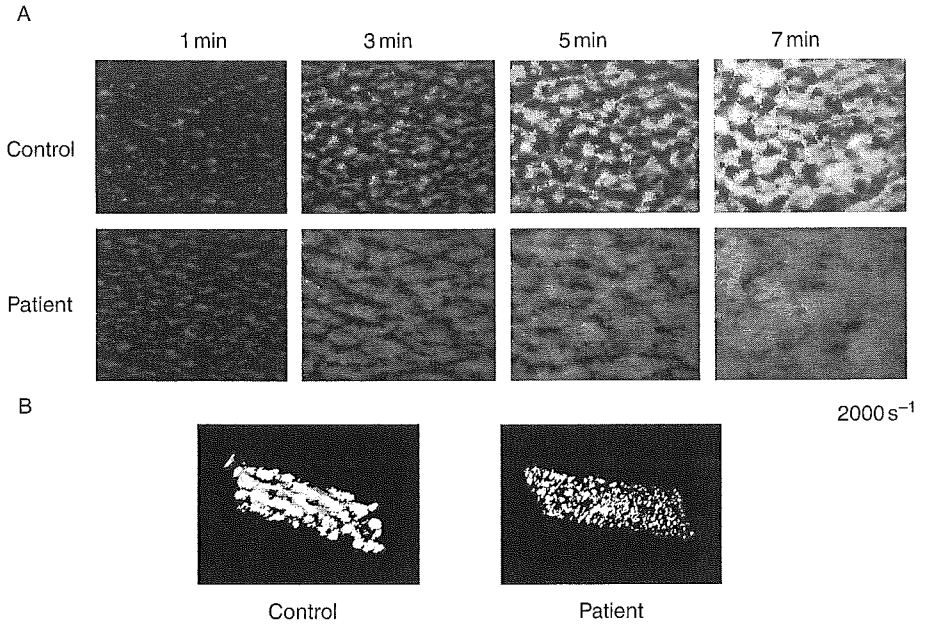

Fig. 7. Thrombus formation on immobilized collagen under flow conditions. (A) Whole blood containing mepacrine-labeled platelets obtained from the patient or control subjects was aspirated through a chamber with type I collagen-coated coverslips. Thrombi formed under a high shear rate (2000 s^{-1}) at indicated time points were observed using a microscope equipped with epifluorescent illumination and a CCD camera system. (B) Three-dimensional structure of thrombi formed after 10 min flow by platelets from the patient or a control subject was analyzed.

binding capacity of 2-methylthioadenosine 5′-diphosphate (2MeS-ADP), was compound heterozygous for Arg256 → Gln in TM6 and for Arg265 → Trp in the third extracellular loop of P2Y$_{12}$. Platelets from patient AC showed an increased platelet aggregation at high dose ADP compared with low dose ADP, suggesting the presence of residual receptor function [16]. In this study, we described a patient (OSP-1) with congenital bleeding diathesis bearing a novel homozygous mutation within the translation initiation codon (ATG → AGG) of the P2Y$_{12}$ gene. Consistent with previous studies, the aggregation of OSP-1 platelets with P2Y$_{12}$ deficiency was impaired to various agonists such as collagen, U46619, and PAR1 TRAP at low concentrations, but almost normal at high concentrations [11–14]. These findings confirmed the critical role of P2Y$_{12}$-mediated signaling evoked by endogenous ADP in platelet aggregation induced by low concentrations of agonists. In contrast to patient AC with residual P2Y$_{12}$-mediated signaling, the impaired platelet aggregation in OSP-1 in response to ADP was neither improved even at 100 μM of ADP stimulation nor reduced by adding 1 μM of AR-C69931MX, suggesting a complete loss of the P2Y$_{12}$ function. Family study confirmed that patient OSP-1 was homozygous for the mutation, and our expression study demonstrated that the mutation is responsible for the P2Y$_{12}$ deficiency.

A number of examples of mutations in the translation initiation codons have been demonstrated in various diseases [24]. Although some cases having mutations in the initiation codons did not express any related abnormal protein, Pattern *et al.* showed an abnormal Gα_s protein possibly synthesized as a result of initiation at downstream ATGs due to a mutation at an initiation codon (ATG → GTG) in patients with Albright's hereditary osteodystrophy [24,25]. In OSP-1, we detected the T → G mutation at position +2, and our expression study denied the possibility that the substitution might induce an alternative translation at downstream ATGs leading to an expression of shorter form of P2Y$_{12}$.

As to platelet spreading onto immobilized fibrinogen, OSP-1 platelets showed the impaired platelet spreading. Similarly, A3P5P inhibited the platelet spreading. It has been well documented that release of endogenous ADP is required for full platelet spreading onto immobilized fibrinogen [23], and Obergfell *et al.* [26] have demonstrated that the platelet spreading requires sequential activation of Src and Syk in proximately to $\alpha_{IIb}\beta_3$. In contrast to the ADP-induced platelet shape change shown in OSP-1 platelets in the platelet aggregometer, our data indicated that both P2Y$_{12}$ and P2Y$_1$ were necessary for the full spreading onto immobilized fibrinogen.

Employing clopidogrel or AR-C69931 MX as an inhibitor for P2Y$_{12}$, several studies examined the role of P2Y$_{12}$ in thrombogenesis under flow conditions [27–30]. However, some discrepancy between the studies was pointed out and non-specific effects of these inhibitors were not completely ruled out [28–30]. As patient OSP-1 was deficient in P2Y$_{12}$ as shown in this study, it would be informative to examine the real-time process of thrombogenesis on a type I collagen-coated surface under a high shear rate (2000 s^{-1}) employing whole blood obtained from OSP-1. Our data demonstrated that P2Y$_{12}$-deficiency led to the loosely packed thrombus and the impaired thrombus growth with enhancing adhesion to collagen, which was consistent with the study by Remijn *et al.* [30] employing patient ML's platelets. The increase in platelet adhesion to

collagen was probably due to the impaired platelet consumption by the growing thrombi [27,30]. Moreover, our real-time observation indicated that the loosely packed aggregates were unable to resist against high shear stress, and then most of the aggregates at the apex of the thrombi came off the thrombi. In contrast, Andre *et al.* [12] did not detect significant differences in *ex vivo* thrombus volume formed over human type III collagen under a shear rate of 871 s^{-1} between $P2Y_{12}^{-/-}$ and WT mice. Although Andre *et al.* used non-anticoagulated mouse blood instead of anticoagulated blood, Roald *et al.* [27] demonstrated that clopidogrel significantly reduced the thrombus volume over type III collagen employing non-anticoagulated human blood. Loosely packed platelet thrombi with swollen non-degranulated platelets were detected following clopidogrel intake, whereas densely packed thrombi with partly fused platelets were detected before clopidogrel intake by electron microscopy [27]. Thus, it is likely that differences between human and mouse, rather than those between non-anticoagulated and anticoagulated blood, may account for the discrepancy. Nevertheless, they showed that *ex vivo* thrombi were loosely packed and that only small and unstable thrombi were formed in $P2Y_{12}^{-/-}$ mice without reaching occlusive size in mesenteric artery injury model *in vivo* [12].

Our present study has demonstrated the novel mutation responsible for the $P2Y_{12}$ deficiency and suggested that secretion of endogenous ADP and subsequent $P2Y_{12}$-mediated signaling is critical for platelet aggregation, platelet spreading, and as a consequence, for stabilization of thrombus. Mild bleeding tendency observed in patient OSP-1 further emphasizes the efficacy of $P2Y_{12}$ receptor as a therapeutic target for thrombosis.

Acknowledgements

We thank Dr Mitsuhiko Sugimoto (Nara Medical University) for his valuable advice to perform the real-time observation of thrombogenesis under flow conditions. This study was supported in part by Grant-in Aid for Scientific Research from the Ministry of Education, Science and Culture in Japan, Grant-in Aid from the Ministry of Health, Labor and Welfare in Japan, Astellas Foundation for Research on Metabolic Disorder, Tukuba, Japan, and Mitsubishi Pharma Research Foundation, Osaka, Japan.

Supplementary material

The following supplementary material is available online at http://www.blackwell-synergy.com/loi/jth:

Figure S1. Perfusion study using control platelets. A real-time movie of platelets perfused over type-I collagen shows that thrombi formed by control platelets are densely packed and stable. This 5-second movie was taken at 5-minute perfusion under a high shear rate (2000 s^{-1}).

Figure S2. Perfusion study using OSP-1 platelets. A real-time movie of platelets perfused over type-I collagen shows that thrombi formed by the patient OSP-1 platelets are loosely packed and unstable. Newly formed aggregates on the top of thrombi keep on moving toward downstream and some aggregates came off the thrombi. This 5-second movie was taken at 5-minute perfusion under a high shear rate (2000 s^{-1}).

References

1 Fuster V, Badimon L, Badimon JJ, Chesebro JH. The pathogenesis of coronary artery disease and the acute coronary syndromes. *N Engl J Med* 1992; **326**: 242–50.

2 Antithrombotic Trialists' Collaboration. Collaborative meta-analysis of randomised trials of antiplatelet therapy for prevention of death, myocardial infarction, and stroke in high risk patients. *BMJ* 2002; **324**: 71–86.

3 Savage B, Almus-Jacobs F, Ruggeri ZM. Specific synergy of multiple substrate–receptor interactions in platelet thrombus formation under flow. *Cell* 1998; **94**: 657–66.

4 Tomiyama Y, Shiraga M, Shattil SJ. Platelet Membrane Proteins as Adhesion Receptors. In: Gresele P, Page C, Fuster V, Vermylen J, eds. *Platelets in thrombotic and non-thrombotic disorders pathophysiology, pharmacology and therapeutics*. Cambridge, UK: Cambridge, 2002: 80–92.

5 CAPRIE Steering Committee. A randomised, blinded, trial of clopidogrel versus aspirin in patients at risk of ischaemic events (CAPRIE). *Lancet* 1996; **348**: 1329–39.

6 Gachet C. ADP receptors of platelets and their inhibition. *Thromb Haemost* 2001; **86**: 222–32.

7 Dorsam RT, Kunapuli SP. Central role of the $P2Y_{12}$ receptor in platelet activation. *J Clin Invest* 2004; **113**: 340–5.

8 Fabre JE, Nguyen M, Latour A, Keifer JA, Audoly LP, Coffman TM, Koller BH. Decreased platelet aggregation, increased bleeding time and resistance to thromboembolism in $P2Y_1$-deficient mice. *Nat Med* 1999; **5**: 1199–202.

9 Leon C, Hechler B, Freund M, Eckly A, Vial C, Ohlmann P, Dierich A, LeMeur M, Cazenave JP, Gachet C. Defective platelet aggregation and increased resistance to thrombosis in purinergic $P2Y_1$ receptor-null mice. *J Clin Invest* 1999; **104**: 1731–7.

10 Hollopeter G, Jantzen HM, Vincent D, Li G, England L, Ramakrishnan V, Yang RB, Nurden A, Julius D, Conley PB. Identification of the platelet ADP receptor targeted by antithrombotic drugs. *Nature* 2001; **409**: 202–7.

11 Foster CJ, Prosser DM, Agans JM, Zhai Y, Smith MD, Lachowicz JE, Zhang FL, Gustafson E, Monsma Jr FJ, Wiekowski MT, Abbondanzo SJ, Cook DN, Bayne ML, Lira SA, Chintala MS. Molecular identification and characterization of the platelet ADP receptor targeted by thienopyridine antithrombotic drugs. *J Clin Invest* 2001; **107**: 1591–8.

12 Andre P, Delaney SM, LaRocca T, Vincent D, DeGuzman F, Jurek M, Koller B, Phillips DR, Conley PB. $P2Y_{12}$ regulates platelet adhesion/activation, thrombus growth, and thrombus stability in injured arteries. *J Clin Invest* 2003; **112**: 398–406.

13 Cattaneo M, Lecchi A, Randi AM, McGregor JL, Mannucci PM. Identification of a new congenital defect of platelet function characterized by severe impairment of platelet responses to adenosine diphosphate. *Blood* 1992; **80**: 2787–96.

14 Nurden P, Savi P, Heilmann E, Bihour C, Herbert JM, Maffran JP, Nurden A. An inherited bleeding disorder linked to a defective interaction between ADP and its receptor on platelets. Its influence on glycoprotein IIb-IIIa complex function. *J Clin Invest* 1995; **95**: 1612–22.

15 Conley P, Jurek M, Vincent D, Lecchi A, Cattaneo M. Unique mutations in the $P2Y_{12}$ locus of patients with previously described defects in ADP-dependent aggregation [abstract]. *Blood* 2001; **98**: 43b. Abstract 3778.

16 Cattaneo M, Zighetti ML, Lombardi R, Martinez C, Lecchi A, Conley PB, Ware J, Ruggeri ZM. Molecular bases of defective signal transduction in the platelet P2Y$_{12}$ receptor of a patient with congenital bleeding. *Proc Natl Acad Sci USA* 2003; **100**: 1978–83.

17 Shiraga M, Tomiyama Y, Honda S, Suzuki H, Kosugi S, Tadokoro S, Kanakura Y, Tanoue K, Kurata Y, Matsuzawa Y. Involvement of Na^+/Ca^{2+} exchanger in inside-out signaling through the platelet integrin $\alpha_{IIb}\beta_3$. *Blood* 1998; **92**: 3710–20.

18 Tomiyama Y, Tsubakio T, Piotrowicz RS, Kurata Y, Loftus JC, Kunicki TJ. The Arg-Gly-Asp (RGD) recognition site of platelet glycoprotein IIb-IIIa on nonactivated platelets is accessible to high-affinity macromolecules. *Blood* 1992; **79**: 2303–12.

19 Honda S, Tomiyama Y, Aoki T, Shiraga M, Kurata Y, Seki J, Matsuzawa Y. Association between ligand-induced conformational changes of integrin $\alpha_{IIb}\beta_3$ and $\alpha_{IIb}\beta_3$-mediated intracellular Ca^{2+} signaling. *Blood* 1998; **92**: 3675–83.

20 Kato H, Honda S, Yoshida H, Kashiwagi H, Shiraga M, Honma N, Kurata K, Tomiyama Y. SHPS-1 negatively regulates integrin $\alpha_{IIb}\beta_3$ function through CD47 without disturbing FAK phosphorylation. *J Thromb Haemost* 2005; **3**: 763–74.

21 Tsuji S, Sugimoto M, Miyata S, Kuwahara M, Kinoshita S, Yoshioka A. Real-time analysis of mural thrombus formation in various platelet aggregation disorders: distinct shear-dependent roles of platelet receptors and adhesive proteins under flow. *Blood* 1999; **94**: 968–75.

22 Honda S, Tomiyama Y, Shiraga M, Tadokoro S, Takamatsu J, Saito H, Kurata Y, Matsuzawa Y. A two-amino acid insertion in the Cys146-Cys167 loop of the α_{IIb} subunit is associated with a variant of Glanzmann thrombasthenia. Critical role of Asp163 in ligand binding. *J Clin Invest* 1998; **102**: 1183–92.

23 Haimovich B, Lipfert L, Brugge JS, Shattil SJ. Tyrosine phosphorylation and cytoskeletal reorganization in platelets are triggered by interaction of integrin receptors with their immobilized ligands. *J Biol Chem* 1993; **268**: 15868–77.

24 Cooper D. Human gene mutations affecting RNA processing and translation. *Ann Med* 1993; **25**: 11–7.

25 Patten J, Johns D, Valle D, Eil C, Gruppuso PA, Steele G, Smallwood PM, Levine MA. Mutation in the gene encoding the stimulatory G protein of adenylate cyclase in Albright's hereditary osteodystrophy. *N Engl J Med* 1990; **322**: 1412–9.

26 Obergfell A, Eto K, Mocsai A, Buensuceso C, Moores SL, Brugge JS, Lowell CA, Shattil SJ. Coordinate interactions of Csk, Src, and Syk kinases with αIIbβ3 initiate integrin signaling to the cytoskeleton. *J Cell Biol* 2002; **157**: 265–75.

27 Roald HE, Barstad RM, Kierulf P, Skjorten F, Dickinson JP, Kieffer G, Sakariassen KS. Clopidogrel - a platelet inhibitor which inhibits thrombogenesis in non-anticoagulated human blood independently of the blood flow conditions. *Thromb Haemost* 1994; **71**: 655–62.

28 Turner NA, Moake JL, McIntire LV. Blockade of adenosine diphosphate receptors P2Y$_{12}$ and P2Y$_1$ is required to inhibit platelet aggregation in whole blood under flow. *Blood* 2001; **98**: 3340–5.

29 Goto S, Tamura N, Handa S. Effects of adenosine 5′-diphosphate (ADP) receptor blockade on platelet aggregation under flow. *Blood* 2002; **99**: 4644–5.

30 Remijn JA, Wu YP, Jeninga EH, IJsseldiik MJ, van Willigen G, de Groot PG, Sixma JJ, Nurden AT, Nurden P. Role of ADP receptor P2Y$_{12}$ in platelet adhesion and thrombus formation in flowing blood. *Arterioscler Thromb Vasc Biol* 2002; **22**: 686–91.

ELSEVIER

EXPERIMENTAL HEMATOLOGY

Experimental Hematology 33 (2005) 495–503

Differential effects of a novel IFN-ζ/limitin and IFN-α on signals for Daxx induction and Crk phosphorylation that couple with growth control of megakaryocytes

Naoko Ishida, Kenji Oritani, Masamichi Shiraga, Hitoshi Yoshida, Sin-ichiro Kawamoto, Hidetoshi Ujiie, Hiroaki Masaie, Michiko Ichii, Yoshiaki Tomiyama, and Yuzuru Kanakura

Department of Hematology and Oncology, Osaka University Graduate School of Medicine, Osaka, Japan

(Received 27 September 2004; revised 23 December 2004; accepted 3 January 2005)

Objective. **Although a novel IFN-ζ/limitin uses IFN-α/β receptor, it lacks some common activities of type I IFNs. We compared effects on megakaryocyte proliferation and differentiation as well as signals for their biological activities.**

Materials and Methods. **Recombinant IFN-ζ/limitin and IFN-α titrated with a cytopathic effect dye binding assay, were used in this study. Colony assays and serum-free suspension cultures for megakaryocytes were performed to compare their growth inhibitory effects. To analyze signals, megakaryocytes cultured in serum-free suspension cultures were stimulated and Western blotted with the indicated antibody.**

Results. **Both IFN-ζ/limitin and IFN-α suppressed the proliferation of megakaryocyte progenitors without influencing their differentiation. However, much higher concentrations of IFN-ζ/limitin were required for the growth inhibition than IFN-α. The growth inhibition by IFN-ζ/limitin and IFN-α was significantly reduced when either Tyk2 or STAT1 was disrupted. In addition, the antisense oligonucleotides against Crk and Daxx, downstream molecules of Tyk2, greatly rescued the IFN-ζ/limitin- and IFN-α-induced reduction of megakaryocyte colony numbers. In cultured megakaryocytes, IFN-ζ/limitin induced the expression of SOCS-1 as strongly as IFN-α. However, IFN-ζ/limitin induced weaker phosphorylation of Crk and lower induction of Daxx than IFN-α.**

Conclusions. **Weaker signals for Crk and Daxx may participate in less megakaryocyte suppressive activity of IFN-ζ/limitin and may distinguish IFN-ζ/limitin from IFN-α in megakaryocytes. Our results extend the understanding about thrombocytopenia in patients with IFN-α treatment as well as the possibility for the clinical application of human homologue of IFN-ζ/limitin or an engineered cytokine with useful features of the IFN-ζ/limitin structure.** © **2005 International Society for Experimental Hematology. Published by Elsevier Inc.**

Introduction

Limitin was initially identified as a growth inhibitor of a myelomonocytic leukemia line with an expression cloning [1]. Limitin shows approximately 30% amino acid sequence identity with interferon (IFN)-α, IFN-β and IFN-ω and recognizes IFN-α/β receptor [1]. It also displays antiviral activity and can induce some effectors as type I IFNs [1,2]. Based on these facts, limitin has been considered as a novel type I IFN with the designation of IFN-ζ by the Nomenclature Committee of the International Society for Interferon and Cytokine Research [3]. Point-by-point comparisons of biological activities between IFN-ζ/limitin and IFN-α have revealed that IFN-ζ/limitin is similar but unique in lacking some common activities of type I IFNs. Similar dose requirement between IFN-ζ/limitin and IFN-α was observed for the enhancement of cytotoxic T lymphocyte activity, the augmentation of MHC class I expression, and the growth inhibition of a myelomonocytic leukemia cell line WEH13 and a murine lymphoblast cell line L1210 [4,5]. However,

Offprint request to: Kenji Oritani, M.D. Ph.D., Department of Hematology and Oncology, Osaka University, Graduate School of Medicine, 2-2 Yamada-oka, Suita, Osaka 565-0871, Japan; E-mail: oritani@bldon.med.osaka-u.ac.jp

0301-472X/05 $–see front matter.
doi: 10.1016/j.exphem.2005.01.002

IFN-ζ/limitin did not suppress colony formation of myeloid and erythroid progenitors, while IFN-α did [1,5]. Much higher concentrations of IFN-ζ/limitin than IFN-α were required for the suppression of colony formation of B lymphocyte progenitors [1,5]. Similarly, approximately 30% of myeloid progenitors and 50% of erythroid progenitors in bone marrow were reduced by IFN-α injections, while there was no influence on these progenitors even when much higher dose of IFN-ζ/limitin was injected [5]. Thus, IFN-ζ/limitin displays similar antiviral, immunomodulatory, and antitumor activities to IFN-α indicating that IFN-ζ/limitin can be utilized for the treatment of diseases where type I IFNs are useful.

The development of megakaryocytes is regulated positively and negatively by a number of growth factors [6]. Thrombopoietin (TPO), interleukin (IL)-3, and granulocyte-macrophage colony-stimulating factor, and stem cell factor augment the proliferation of megakaryocyte progenitors [7]. TPO, IL-6, IL-11, and leukemia inhibitory factor promote the polyploidization and cytoplasmic maturation of megakaryocytes. In contrast, transforming growth factor-β1 and some CXC chemokines suppress the proliferation of megakaryocytes [8,9]. IFN-α and IFN-γ also act as negative regulators of megakaryopoiesis [10,11]. Thus, clarification of precise mechanisms of growth inhibitory effects on megakaryocyte progenitors by IFNs is important to develop new strategies for the improved IFN therapy [12]. In this study, we investigated the growth inhibitory effects of IFN-ζ/limitin and IFN-α on megakaryocytes and compared the molecular basis of their effects by using bone marrow cells derived from knockout mice and the recently established culture system for megakaryocytes [13–15]. Our results indicate that IFN-ζ/limitin has fewer megakaryocyte-suppressive properties than IFN-α and that both Tyk2- and STAT1-dependent pathways participate in the growth inhibitory effects of IFNs. While gene expression of SOCS-1 was induced similarly, IFN-ζ/limitin induced lower expression of Daxx and weaker phosphorylation of Crk than IFN-α. These different signals may explain why IFN-ζ/limitin exhibits less growth suppressive effects than IFN-α on megakaryocyte progenitors.

Materials and methods

Cytokines and antibodies

Recombinant IFN-ζ/limitin was produced and purified as described in our previous articles [2,16]. Its purity was more than 98% when evaluated by gel filtration chromatography. Recombinant murine IFN-α was purchased from HyCultBiotech (Uden, Netherlands). Both IFN-ζ/limitin and IFN-α were titrated with cytopathic effect dye uptake method where L929 cells were infected with encephalomyocarditis virus, and each specific activity was determined by a comparison with a standard IFN-α which was provided from the National Institutes of Health.

Antibodies against Daxx and Crk as well as an anti-phosphotyrosine antibody were purchased from Santa Cruz Biotechnology (Santa Cruz, CA, USA). Anti- Tyk2, STAT1, STAT5, and ERK1/2 as well as antibodies against their phosphorylated forms were also purchased from Santa Cruz Biotechnology. Fluorescein isothiocyanate (FITC)-conjugated rat anti-mouse αIIb/CD41 antibody, phycoerythrin (PE)-conjugated anti-mouse CD11b, CD45R, CD3, TRE119 antibodies were purchased from Pharmingen (San Diego, CA, USA).

Mice

C57BL/6 mice were purchased from Japan Clea (Tokyo, Japan). Tyk2-deficient mice were provided by Dr. Shimoda (Kyushu University, Fukuoka, Japan) [17]. STAT1-deficient mice were a kind gift from Dr. Kaisho (Osaka University, Osaka, Japan) [18], and IRF-1-deficient mice from Dr. Taniguchi (Tokyo University, Tokyo, Japan) [19]. All mice were maintained at the Institute for Experimental Animals, Osaka University School. Mice were approximately 6 to 10 weeks of age at the time of use.

Suspension cultures for megakaryocytes

Bone marrow cells were harvested by flushing femurs and tibias with phosphate-buffered saline (PBS) containing 2% bovine serum albumin (Sigma, St. Louis, MO, USA), 0.38% trisodium citrate, and 1 U/mL DNase. Mononuclear cells were isolated over Lymphoprep (Fresenius Kabi norge AS, Oslo, Norway) after a 30-minute centrifugation at 400g. The low-density mononuclear cells (10^6 cells/mL) were cultured for 5 days in Iscove's modified Dulbecco's medium (GIBCO, Grand Island, NY, USA) supplemented with 200 μg/mL human transferrin (Sigma), 5 mg/mL bovine serum albumin, and 10 μg/mL human insulin (Sigma), together with 10 ng/mL murine thromboporetin (TPO; a gift from Kirin Brewery Ltd., Japan), and 10 ng/mL human IL-11 (Yamanouchi Pharmaceutical Co., Ltd., Osaka, Japan).

Clonal proliferation of megakaryocytes (CFU-Meg)

Bone marrow mononuclear cells (10^5/dish) were suspended in 1 mL of MegaCult-C collagen-based system (Stem Cell Technologies, Vancouver, British Columbia, Canada) composed of Iscove's modified Dulbecco's medium, 0.9% methylcellulose, 100 μM 2-mercaptoethanol, 2 mM L-glutamine, 1% bovine serum albumin, 1.1 mg/mL collagen with 50 ng/mL TPO and 50 ng/mL IL-11. Numbers of colonies were counted on day 7, and megakaryocytes in the generated colonies were confirmed by the staining for the acetylcholinesterase activity. In some experiments, bome marrow cells were stained with the mixture of PE-conjugated anti-mouse CD11b, CD45R, CD3, TRE119 antibodies, and the lineage-negative cells were sorted with FACStar Plus (Becton-Dickinson, San Jose, CA, USA). The sorted cells were used as a source of CFU-Meg colony assays.

Flow cytometry

Antibody incubations and washing steps were accomplished on ice in PBS containing 1% bovine serum albumin and 0.1% sodium azide. The stained cells were analyzed with FACSort (Becton-Dickinson). To analyze the DNA ploidy, cultured megakaryocytes were suspended in 100 μL of PBS, and fixed by the addition of 900 μL of cold ethanol. The fixed cells were incubated with 300 μL of staining buffer (1 μg/mL RNase, 20 μg/mL propidium iodide, and 0.01% NP-40 in PBS) at 37°C for 10 minutes. The DNA contents in the nucleus of the cells were analyzed with FACSort using Cell Quest software. To detect apoptotic cells, annexin V staining was performed using a BD ApoAlert Annexin

V kit (BD Biosciences, Palo Alto, CA, USA). Briefly, cells were washed twice with PBS and resuspended in 200 μL of binding buffer containing 5 μL of annexin V and 10 μL of propidium iodide for 15 minutes at room temperature. The cells were then rinsed and analyzed with FACSort.

Western blot

Cultured megakaryocytes were serum-starved, stimulated with IFN-ζ/limitin or IFN-α for the indicated period, and then lysed in lysis buffer (10 mM Tris-HCl pH 7.5, 1% NP-40, 0.1% sodium dodecyl sulfate, 150 mM NaCl, 1 mM EDTA, 10% aprotinin, 1 mM PMSF, 100 μg/mL leupeptin, 100 mM Na_3VO_4), followed by centrifugation at 10,000g for 10 minutes. For immunoprecipitation, the lysates, which were obtained from 10^7 cells, were incubated with the indicated antibodies, followed by the addition of protein G sepharose beads (Amersham, Arlington Heights, IL, USA) for 2 hours at 4°C. The whole-cell lysates (10% of cell lysates) or the immunoprecipitates were subjected to sodium dodecyl sulfate–polyacrylamide gel electrophoresis. The proteins were electrophoretically transferred onto a polyvinylidene difluoride membrane (Immobilion; Millipore Corp., Bedford, MA, USA). After blocking of residual binding sites on the filter, immunoblotting was performed with the appropriate antibodies. Immunoreactive proteins were visualized with the enhanced chemiluminescence detection system (DuPont NEN, Boston, MA, USA).

Northern blot

Total RNAs were isolated using TRIzol Reagent (GIBCO). The RNAs were electrophoresed through a formaldehyde agarose gel and transferred onto a nylon membrane (Amersham). The cDNA fragments were labeled with ^{32}P-dCTP using a random primed DNA labeling kit (Boehringer Mannheim, Indianapolis, IN, USA) and hybridized to the membrane. Blots were then washed and autoradiographed. The cDNA fragments of SOCS-1, Daxx, and β-) actin genes were used as probes [1,20].

Results

IFN-ζ/limitin has less megakaryocyte suppressive properties than IFN-α

We previously reported that IFN-ζ/limitin was unique in no or little influence on the proliferation of normal myeloid, erythroid, and lymphoid cells [1,2]. To compare effects on megakaryopoiesis between IFN-ζ/limitin and IFN-α, CFU-Meg colony assay was employed in the presence of either IFN-ζ/limitin or IFN-α, Both IFN-ζ/limitin and IFN-α inhibited clonal proliferation of megakaryocyte progenitors in a dose-dependent manner (Fig. 1A). The growth inhibition by IFN-α was evident at 5 IU/mL, and only 17.7% of CFU-Meg colonies as compared with control cultures were generated at 2000 IU/mL. However, the cloning efficiency of CFU-Meg was only slightly decreased by the addition of IFN-ζ/limitin (57.5 ± 0.5 with IFN-ζ/limitin, 16.5 ± 1.5 with IFN-α per 10^5 bone marrow cells at the concentration of 2000 IU/mL). Because semisolid cultures of whole bone marrow cells contained numerous accessory cells, which could mediate the IFN effects, we then subsequently used purified megakaryocyte progenitor populations. Similarly to the results using whole bone marrow cells, IFN-ζ/limitin exhibited less reduction of CFU-Meg colonies generated from lineage-negative cells than IFN-α (Fig. 1B). In addition, the weak suppression of CFU-Meg colony formation by IFN-ζ/limitin was completely canceled by the addition of anti-IFN-ζ/limitin polyclonal antibody (data not shown). Serum-free cultures of bone marrow cells in the presence of TPO and IL-11 arose a large number of megakaryocytes [15]. While both IFN-ζ/limitin and IFN-α reduced the numbers of viable cells and αIIb/CD41$^+$ cells, the inhibition by IFN-ζ/limitin was smaller than that by IFN-α (Fig. 2A and B). After megakaryocytes were produced in serum-free cultures for 5 days, the generated megakaryocytes were collected and recultured for an additional 3 days to analyze effects of IFN-ζ/limitin and IFN-α on their proliferation and apoptosis. The recovered cell number was significantly reduced by the addition of IFN-α, but only a small difference was observed between control and IFN-ζ/limitin-containing cultures (Fig. 2C). When apoptotic cells were evaluated with annexin V staining, which detected phosphatidylserine present in the outer membrane of apoptotic cells, the addition of IFN-ζ/limitin and IFN-α did not change the proportion of annexin V$^+$ cells (data not shown). Therefore, both IFN-ζ/limitin and IFN-α directly exhibit cytostatic effects on megakaryocyte progenitors, but IFN-ζ/limitin displays much less megakaryocyte-suppressive activity than IFN-α.

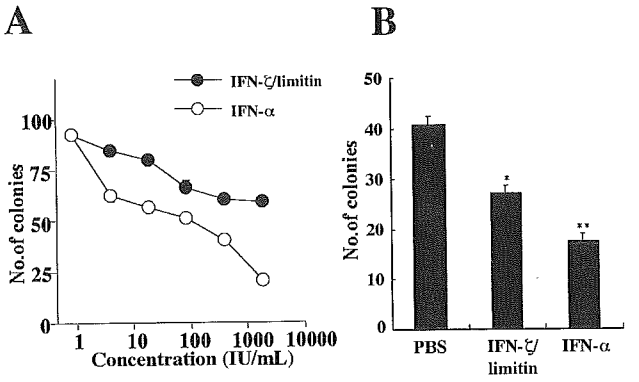

Figure 1. Effects of interferon (IFN)-ζ/limitin and IFN-α on CFU-Meg colony formation. Bone marrow mononuclear cells (1 X 10^5 cells/dish) **(A)** or purified lineage-negative cells (5 X 10^3 cells/dish) **(B)** were cultured in MegaCult -C collagen-based systems with the indicated concentrations of IFN-ζ/limitin (closed square) or IFN-α (open square), and CFU-Meg colony formation was estimated on day 7. The results represent mean ± SD of triplicate cultures. Statistically significant differences from control values are indicated by one ($p<0.05$) or two ($p<0.01$) asterisks. Similar results were obtained in six independent experiments.

Neither IFN-ζ/limitin nor IFN-α affect the differentiation of megakaryocytes

The cultured cells in serum-free medium increased cell size within 5 days and were divided into three groups [15]. As shown in Figure 3A, the percentages of each population were 3.7% (Gate L), 27.2% (Gate M), and 69.0% (Gate S) in control cultures. Both IFN-ζ/limitin and IFN-α did not

alter the proportion of the three groups. When the cultured cells were analyzed for αIIb/CD41 expression as a marker of megakaryocyte differentiation, approximately 80% of cells were αIIb/CD41$^+$ in control cultures (Fig. 3B). Similarly, 80.5% and 81.7% of the cultured cells in the presence of IFN-ζ/limitin or IFN-α expressed αIIb/CD41. DNA ploidy of the Gate S population was 2N in all types of cultures (data not shown). DNA ploidy of the Gate L population ranged from 8 to 64 N in control cultures, and similar results were observed in IFN-ζ/limitin- or IFN-α-containing cultures (Fig. 3C). Therefore, both IFN-ζ/limitin and IFN-α have no effects on megakaryocyte differentiation.

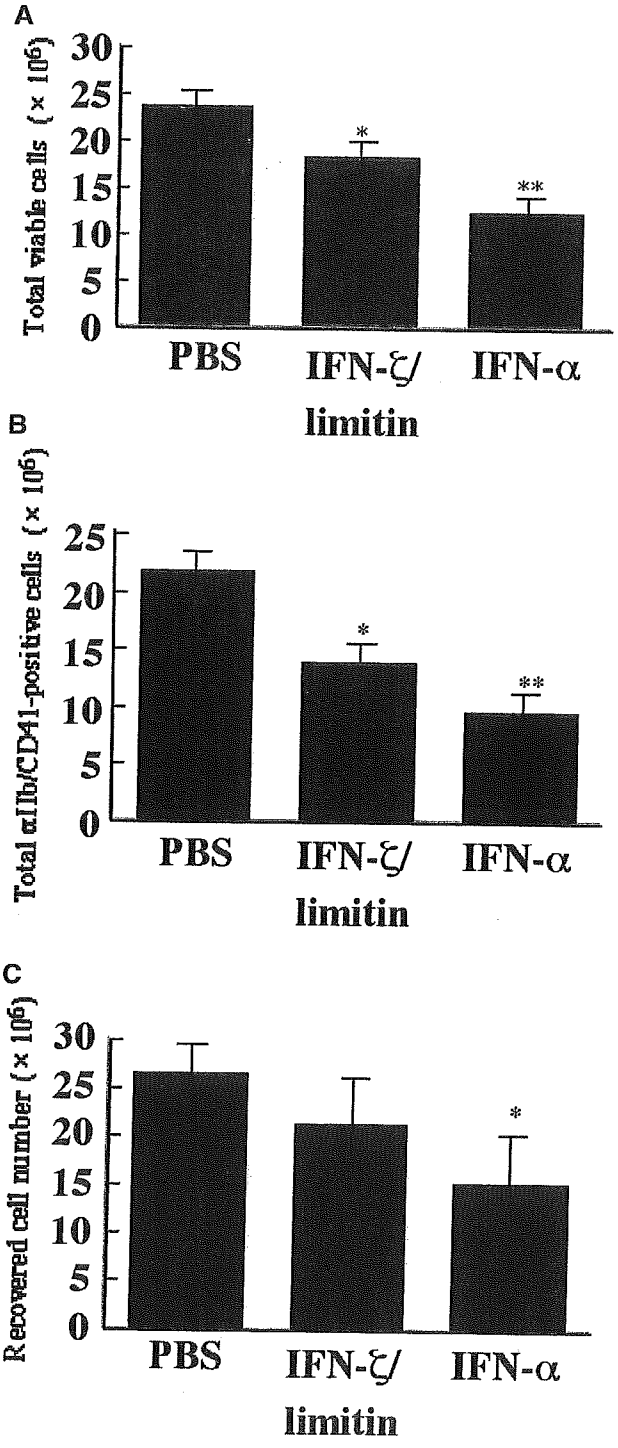

Both Crk and Daxx are required for the IFN-ζ/limitin- and IFN-α-induced growth inhibition of megakaryocyte progenitors

A major pathway for IFN signals involves the activation of tyrosine kinases of Jaks and STATs proteins [21]. To determine what signals are important for the suppression of megakaryopoiesis by IFN-ζ/limitin and IFN-α, we performed CFU-Meg colony assays using bone marrow cells derived from several knockout mice. IFN-ζ/limitin and IFN-α reduced the numbers of colonies up to 67% and 33% in wild-type mice, respectively (Fig. 4). Similar reduction was observed when bone marrow cells derived from IRF-1-deficient mice were used for the assays. In contrast, the destruction of Tyk2 or STAT1 resulted in the significant cancellation of IFN-ζ/limitin-and IFN-α-induced inhibition of CFU-Meg colony formation. Therefore, both Tyk2 and STAT1 play a role in IFN-ζ/limitin- and IFN-α-induced reduction of CFU-Meg colony numbers.

SOCS-1, whose gene expression is induced by some STATs including STAT1, is known to inhibit the proliferation of megakaryocyte progenitors via blunting TPO-induced signals in IFN-α-treated megakaryocytes [11]. IFN-α-induced growth inhibition was mainly mediated by Crk in myeloid and erythroid progenitors, and by Daxx in B lymphocyte progenitors [20,22,23]. We investigated role of Crk and Daxx, downstream molecules of Tyk2, in IFN-ζ/limitin- and IFN-α-induced growth inhibition of megakaryocyte progenitors. As shown in Figure 5A, the protein expression of Daxx and Crk was under detectable levels after the treatment with their antisense oligonucleotides. The reduction of CFU-Meg colony numbers was great canceled by the addition of

Figure 2. Effects of interferon (IFN)-ζ/limitin and IFN-α on the production of megakaryocytes in serum-free suspension cultures. **(A, B):** Bone marrow mononuclear cells (1 X 10^6 cells/mL) were cultured in serum-free conditioned medium with 10 ng/mL thrombopoietin (TPO) and 10 ng/mL IL-11 in the presence of 500 IU/mL of the indicated IFNs. After 5 days of culture, the numbers of viable cells **(A)** as well as αIIb/CD41$^+$ cells **(B)** were estimated. The results represent mean ± SD of triplicate cultures. Similar results were obtained in five independent experiments. **(C):** After bone marrow mononuclear cells (1 X 10^6 cells/mL) were cultured in serum-free conditioned medium with 10 ng/mL TPO and 10 ng/mL IL-11 for 5 days, the viable cultured megakaryocytes (1 X 10^3 cells/well) were collected and recultured with 10 ng/mL TPO and 10 ng/mL IL-11 in the presence of 500 IU/mL of IFN-ζ/limitin or IFN-α for additional 3 days. The recovered cells were counted with a hemocytometer. The results represent mean ± SD of triplicate cultures. Statistically significant differences from control values are indicated by one ($p<0.05$) or two ($p<0.01$) asterisks.

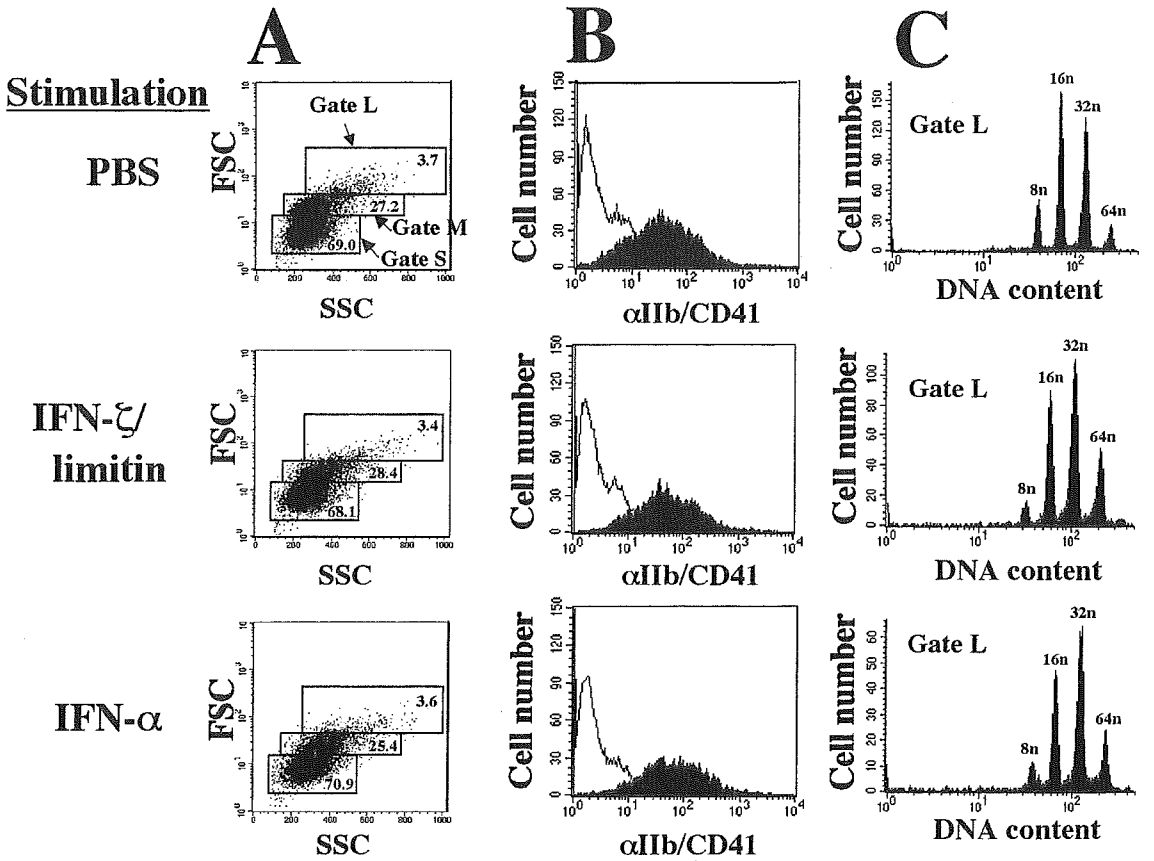

Figure 3. Neither IFN-ζ/limitin nor IFN-α influenced the differentiation of megakaryocytes. Bone marrow mononuclear cells (1 X 10^6 cells/mL) were cultured in serum-free conditioned medium with 10 ng/mL TPO and 10 ng/mL IL-11 in the presence of 1000 IU/mL IFN-ζ/limitin or IFN-α for 5 days. The whole cultured cells were subjected to flow cytometry analysis for cell sizes (**A**) and the αIIb/CD41 expression (**B**). The large cell population (Gate L) of the cultured cells were analyzed for their DNA ploidy (**C**). Each figure shows one of four similar experiments.

these antisense, but not sense, oligonucleotides (Fig. 5B; 84.1% ± 4.8% cancellation with Daxx antisense, 76.4% ± 4.8% cancellation with Crk antisense in the presence of IFN-ζ/limitin; 73.9% ± 6.1% cancellation with Daxx antisense, 81.6% ± 0.1% cancellation with Crk antisense in the presence of IFN-α. Therefore, both Daxx and Crk are important for IFN-ζ/limitin- and IFN-α-induced reduction of CFU-Meg colony numbers.

IFN-ζ/limitin induces lower Daxx expression and weaker Crk phosphorylation than IFN-α in megakaryocytes

As shown in Figure 3, most of the cultured cells in serum-free suspension cultures expressed αIIb/CD41. Thus, we next analyzed some signals induced by IFN-ζ/limitin and IFN-α by using the cultured megakaryocytes. When IFN-ζ/limitin and IFN-α were added to the TPO-containing megakaryocyte cultures for the last 24 hours of the culture period, they did not alter the phosphorylation levels of ERK1/2 or STAT5, which are downstream events of TPO signaling (Fig. 6). We also compared direct signals for STAT1, Tyk2, SOCS-1, Daxx, and Crk induced by IFN-ζ/limitin and IFN-α after the cultured megakaryocytes were starved from cytokines. While IFN-ζ/limitin and IFN-α induced similar levels of the phosphorylation of STAT1, IFN-ζ/limitin induced weaker phosphorylation of Tyk2 than IFN-α (Fig. 7A). IFN-ζ/limitin and IFN-α induced similar level of the gene expression of SOCS-1 (Fig. 7B). Although both IFN-ζ/limitin and IFN-α induced the protein and gene and protein expression of Daxx and the phosphorylation of Crk, their induction by IFN-ζ/limitin was significantly weaker than IFN-α (Fig. 7B and C). Therefore, IFN-ζ/limitin might be unique in lower Daxx induction and weaker Crk phosphorylation in megakaryocytes as compared with IFN-α.

Discussion

IFN-α and IFN-β are widely utilized for the treatment of patients with virus infection, autoimmune diseases, and malignant diseases [24]. Recent advances for IFN therapy are a combined therapy with ribavirin as well as an appearance of a pegylated IFN and a consensus IFN [25–27]. Although these new therapeutic strategies are more efficient than IFN

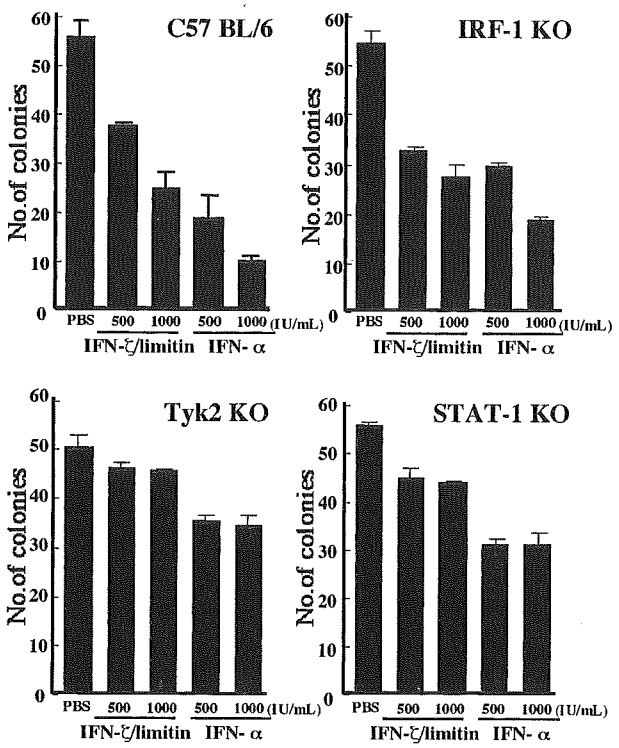

Figure 4. Both Tyk2- and STAT1-dependent pathways are required for the IFN-ζ/limitin- and IFN-α-induced inhibition of CFU-Meg colony formation. Bone marrow mononuclear cells (1 X 10^5 cells/dish) derived from wild-type, IRF-1-deficient, Tyk2-deficient, and STAT1-deficient mice were cultured in MegaCult -C collagen-based systems with 500 or 1000 IU/mL IFN-ζ/limitin or IFN-α, and CFU-Meg colony formation was estimated on day 7. The results represent mean colony numbers ± SD of triplicate cultures. Similar results were obtained in four independent experiments.

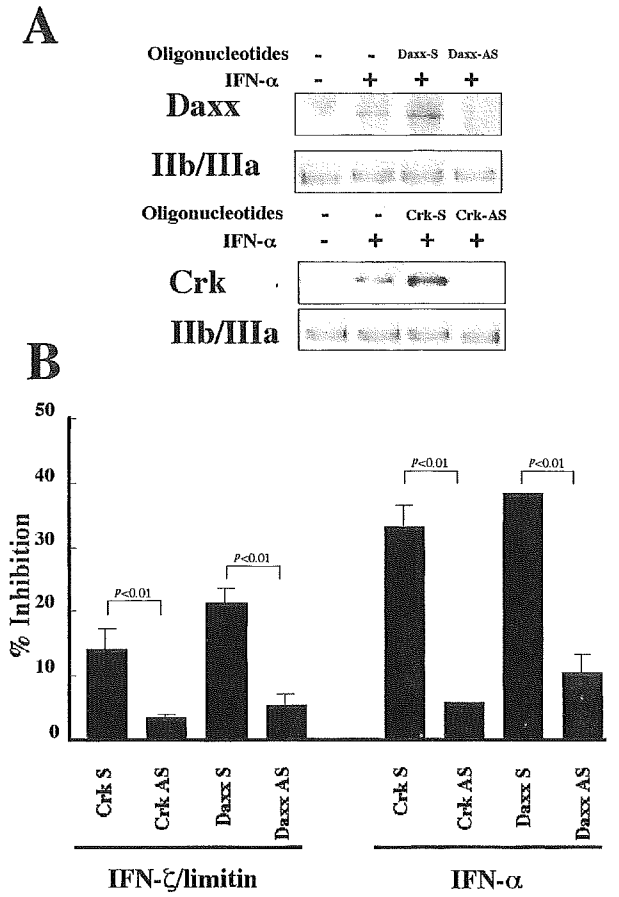

Figure 5. Both Daxx and Crk are required for the IFN-ζ/limitin- and IFN-α-induced inhibition of CFU-Meg colony formation. **(A):** Megakaryocytes (1 X 10^6 cells/well) in serum-free suspension cultures were treated with 280 μg/mL of the indicated oligonucleotides for 8 hours. Their whole cellular lysates (10%) were Western blotted with the indicated antibodies. **(B):** Bone marrow mononuclear cells (1 X 10^5 cells/dish) were preincubated with the indicated oligonucleotides for 8 hours, and then cultured in MegaCult -C collagen-based systems in the presence of 500 IU/mL IFN-ζ/limitin or IFN-α, and CFU-Meg colony formation was estimated on day 7. The data show mean ± SD percentages of inhibition in four independent experiments. Control (with PBS) colony numbers ranged from 106 to 112. The sequences of the phosphothionate oligonucleotides used here were as follows: Daxx-S (5′-GAACCCCCATGGCCACCG-3′), Daxx-AS (5′-CGGTGGCCATGG GGGTTC-3′), Crk-S (5′-CCAACACCATGTCCTCCG-3′), and Crk-AS (5′-CGGAGGACATGGTGTTGG-3′). % inhibition for each oligonucleotide was calculated as [1 – (colony number with IFN-ζ/limitin or IFN-α) / (colony number with PBS)] x 100. Statistically significant differences from results for sense oligonucleotides are indicated.

monotherapy, adverse effects of IFNs are still severe problems. Thus, it is particularly exciting to find a novel IFN with uniquely narrow range of functions and targets that lead to the reduction of adverse effects. In the current study, we found that both IFN-ζ/limitin and IFN-α suppressed the proliferation of megakaryocyte progenitors without influencing megakaryocyte differentiation. However, much higher concentrations of IFN-ζ/limitin were required for the growth suppression of megakaryocyte progenitors than IFN-α. Taken together with our previous data that much higher concentrations of IFN-ζ/limitin were required for the growth suppression of myeloid, lymphoid, and erythroid progenitors [1,2], IFN-ζ/limitin could be superior to IFN-α and IFN-β in clinical utility because of less adverse effects on normal lympho-hematopoietic progenitors.

The available information suggests that IFNs cause clustering of IFN-α/β receptor [28], resulting in phosphorylation of the receptor as well as two Jaks (Jak1 and Tyk2) and some STAT proteins. The phosphorylated STAT1-STAT2 complexes combine with IFN regulatory factor (IRF)-9, known as IFN-stimulated gene factor 3 (ISGF3), and migrate to the nucleus where they bind to the IFN-stimulated response element (ISRE) [29]. Another important pathway is mediated by STAT1-STAT1 homodimer that binds to IFN-γ activated sequence (GAS sequence), leading to the induction of IRF-1 [30]. On the other hand, an adaptor protein Crk is directly associated with Tyk2 and its IFN-α-induced phosphorylation is mediated by Tyk2 [31]. The IFN-α-induced expression and translocation of a nuclear protein Daxx